NASA Contractor Report 191017

STRUCTURAL TAILORING OF ADVANCED TURBOPROPS (STAT)

Theoretical Manual

K. W. Brown

United Technologies Corporation
Pratt & Whitney
400 Main Street
East Hartford, Connecticut 06108

October 1992

Prepared for
Lewis Research Center
Under Contract NAS3–23941

National Aeronautics and
Space Administration

UNITED TECHNOLOGIES
PRATT & WHITNEY

In reply, please refer to:
ET:ds:MS 163-09
Ref. No. PWA-5767-109, NASA CR-191017

March 26, 1993

To: National Aeronautics and Space Administration
Lewis Research Center
21000 Brookpark Road
Cleveland, Ohio 44135

Attention: Mr. Dale Hopkins, Program Manager
Mail Stop 49-8

Subject: Structural Tailoring of Advanced Turboprops (STAT) Theoretical Manual

Reference: Contract NAS3-23941

Enclosures: Three Copies of Subject Report, NASA CR-191017

We are pleased to submit the STAT Theoretical Manual, in compliance with the terms of the referenced contract.

Sincerely yours,

UNITED TECHNOLOGIES CORPORATION
Pratt & Whitney Group

E. S. Todd

E. S. Todd
Program Manager

cc: Administrative Contracting Officer
Defense Plant Representative Office
UTC/Pratt & Whitney Group
East Hartford, Connecticut 06108

TABLE OF CONTENTS

TABLE OF CONTENTS (continued)

LIST OF FIGURES

LIST OF FIGURES (continued)

LIST OF TABLES

1. STAT PROGRAM DESCRIPTION

The Structural Tailoring of Advanced Turboprops (STAT) computer program was developed to perform numerical optimizations on highly swept counter-rotating propfan stages. The optimization procedure seeks to minimize an objective function, defined as either direct operating cost or aeroelastic differences between a blade and its scaled model, by tuning internal and external geometry variables that must satisfy realistic blade design constraints.

The STAT analyses include an aerodynamic efficiency evaluation, a finite element stress and vibration analysis, an acoustic analysis, a flutter analysis, and a once-per-revolution (one-p) forced response life prediction capability. The STAT constraints include blade stresses, blade resonances, flutter, tip displacements and a one-p forced response life fraction. The STAT variables include all blade internal and external geometry parameters needed to define a composite material blade. The STAT objective function is dependent upon a blade baseline definition which the user supplies to describe a current blade design for cost optimization or for the tailoring of an aeroelastic scale model.

To perform a blade optimization, three component analysis categories are required: an optimization algorithm; approximate analysis procedures for objective function and constraint evaluation; and refined analysis procedures for optimum design validation. The STAT computer program contains an executive control module, an optimizer, and all necessary component analyses. The optimization algorithm of STAT is the Automated Design Synthesis (ADS) optimization package, which is a proven tool for optimizations with a small to medium (1 to 30) number of design variables. A flowchart of the STAT procedure is shown in Figure 1.

The structural analysis of STAT utilizes an efficient, coarse mesh, plate finite element blade vibration analysis procedure. The finite element analysis provides blade natural frequencies and mode shapes, stress under centrifugal and pressure loads, and blade weight. Additional constraint evaluations, including flutter, power, acoustic and one-p calculations, utilize outputs from the finite element analysis.

To use the blade optimization system, curves used to describe the external and internal geometry of each turboprop rotor are defined. External geometry curves define blade thickness, section stacking, camber, chord, twist and conical sections. Internal geometry curves define individual layer thickness, percent chord coverage and position over the blade planform.

The STAT system has been applied to both single rotation propfans (SRP) and counter rotation propfans (CRP). SRP applications include the Large-Scale Advanced Prop-fan (LAP) SR-7 blade, the LAP SR-7 aeroelastic scale model blade and the 18E SR-7 infeasible blade design. CRP applications include development of the first analytically feasible full-scale rotor, CRPX1, and the development of an aerodynamic scale model of this new rotor system. The STAT program made significant improvements in all cases and demonstrated the great potential for design enhancements through the application of numerical optimization to turboprop fan blades of composite construction.

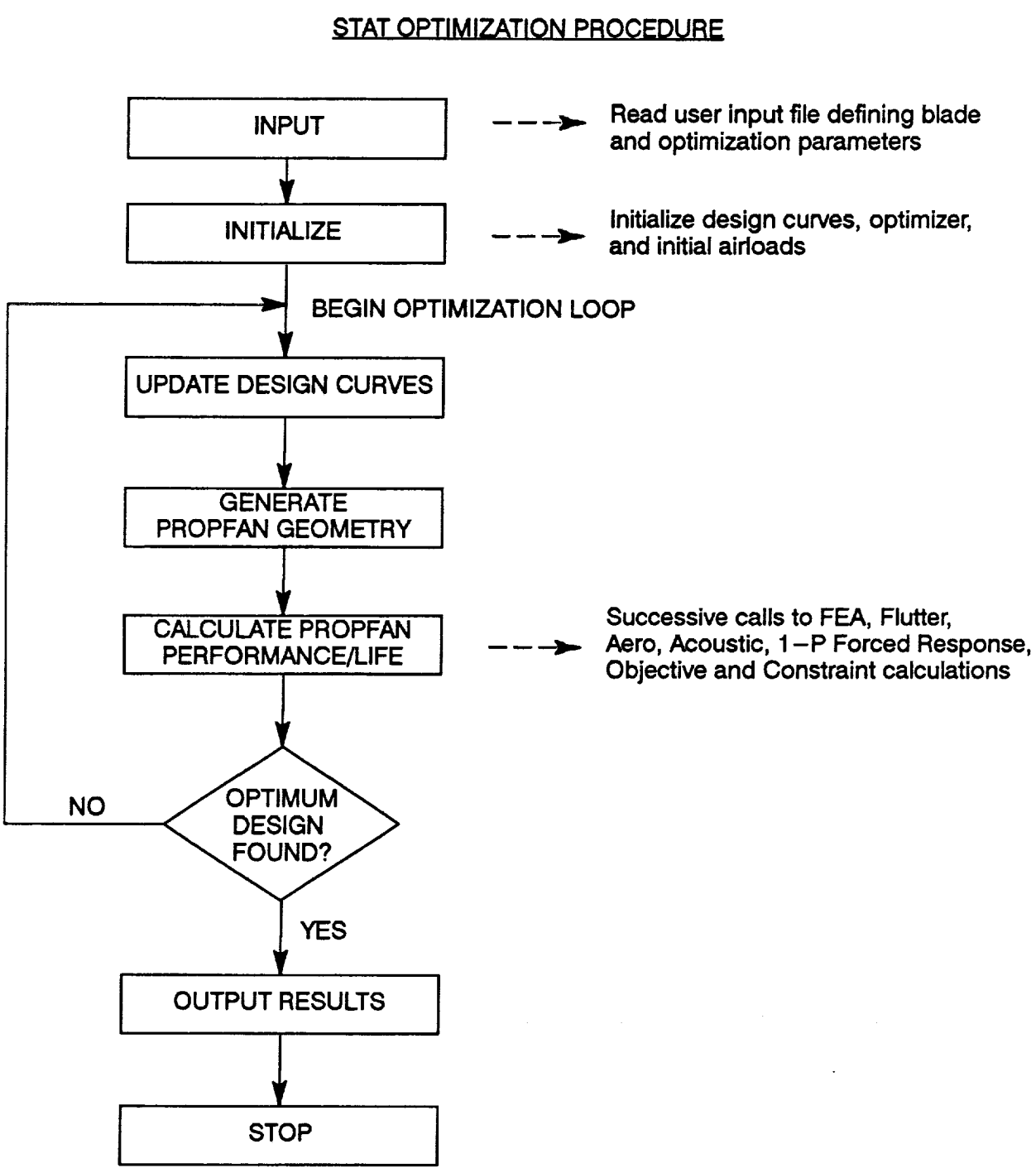

Figure 1. Structural Tailoring of Advanced Turboprops Overall Program Flow

2. OPTIMIZATION PROCEDURES

To perform a successful blade optimization requires intelligent updating of many design parameters, and many applications of detailed analysis procedures. To meet this challenge, STAT has been assembled using the most efficient analysis procedures obtainable (Section 3), as well as the most efficient optimization algorithms.

Conventional optimization procedures work well with a small to medium number of design variables (Reference 1). Approximation techniques, such as quadratic regressions, work well with up to six or eight design variables. Beyond this number of design parameters, direct methods, such as the method of feasible directions, are preferred. Direct methods work acceptably with up to 40 or 50 design variables.

For a complicated optimization like the design of counter-rotating propfans, hundreds of design parameters are available. To ensure that STAT employed a reasonable number of design variables so that conventional optimization procedures would be applicable, the concept of design curves was developed.

The design curve concept recognizes that most propfan airfoil parameters, such as airfoil chord and thickness, are normally defined as functions of the radius. Thus, while each section may have a unique thickness, many of these parameters may be linked together via a single "curve." Within STAT, each design curve may be continuously updated via the selection of design variables at selected radial locations. As a single parameter value is updated, the curves are resplined, thus effecting the value of the parameter at many radial stations. In this fashion, STAT gives the user a great degree of design flexibility, while minimizing the number of design variables required in an optimization.

The optimization algorithm of STAT is the ADS (Reference 2) optimization package. ADS offers a wide variety of optimization procedures and is a well accepted and proven optimization tool for optimizations with a small to medium (1 to 30) number of design variables.

In most optimizations, the efficiency and reliability of the numerical optimization process may be enhanced by scaling of the design variables. Indeed, the ADS optimizer has such a capability built into its procedure. Unfortunately, due to the way that STAT's design curves are defined, the ADS scaling procedure is rendered ineffective. To counter this problem, a design scaling algorithm has been included within the STAT program.

2.1 STAT Design Curves

The complete structural definition of a stage requires the effective processing of many design parameters. For the blade definition, blade descriptive information is input through design curves, in which blade geometric parameters are tabulated as functions of an abscissa, in this case the section percent span. These tabulated values are stored as splines, so that a design data base is available, with section information available at any number of stations.

The airfoil external geometry is defined through thickness/chord, chord/diameter, stacking x,y,z points/radius, section cone angles, twist angles and a nondimensional camber/lift coefficient parameter. The airfoil composite internal construction is defined through wall thickness, percent chord coverage, and percent chord meanline curves.

To provide design freedom and generality, STAT supports all of these blade geometry parameters as design variables. By allowing the analyst to select the number of design variables he/she wants to use in the radial direction for any particular design curve, STAT permits the analyst to tailor the flexibility of the design optimization, while maintaining effective run times. Present experience has shown design tailoring success with over 40 design variables used.

Design Data Curves

In STAT, except for a few discrete quantities such as the attachment geometry, aerodynamic environment and material properties, all design data are stored in tabular form as splines of the design curves. The design curves are defined in the program as data values with a corresponding abscissa, usually but not necessarily the section radius. The structural and fabrication data necessary to describe the blade internal and external geometry are stored in these design tables. Using quintic spline algorithms, design curve reference is available, so that any curve may be referenced at any arbitrary required radial location.

As the design optimization process commences, it is necessary for STAT to update the design curves to reflect the present analysis geometry. Thus, two sets of design curves are maintained – an original set of curves, and a current set. The baseline design curves are updated via design curve increments. A detailed definition of the curve increments is determined via a spline fit of available design variables. Thus, any curve may be updated by having one or more design variables assigned to it. The variable curve is splined, then added to the baseline curve, thus creating the current design curve, from which the analysis geometry is derived, as shown in Figure 2.

By using the curve incrementing procedure, several advantages are obtained. First, it is always possible to reproduce a baseline design. If the design variables are the curve values themselves, rather than increments, it is difficult to regenerate an accurate baseline geometry without an inordinate number of design variables. By splining increments of baseline curves, a design variable set of zeroes always exactly reproduces the original design. Secondly, the process allows for reducing the optimizer design variable requirements by providing for dependent variables and for constant terms. A dependent variable assignment allows for a curve to be incremented at several abscissa locations even though it may have only one design variable attributed to it. Dependent variables are incremented in user prescribed ratios to the actual design variables, and are unknown to the optimizing algorithm itself. The provision of a constant term allows a curve location to be held to a constant value, including a prescribed increment. This capability, therefore, provides the user the ability to perform a restart optimization analysis.

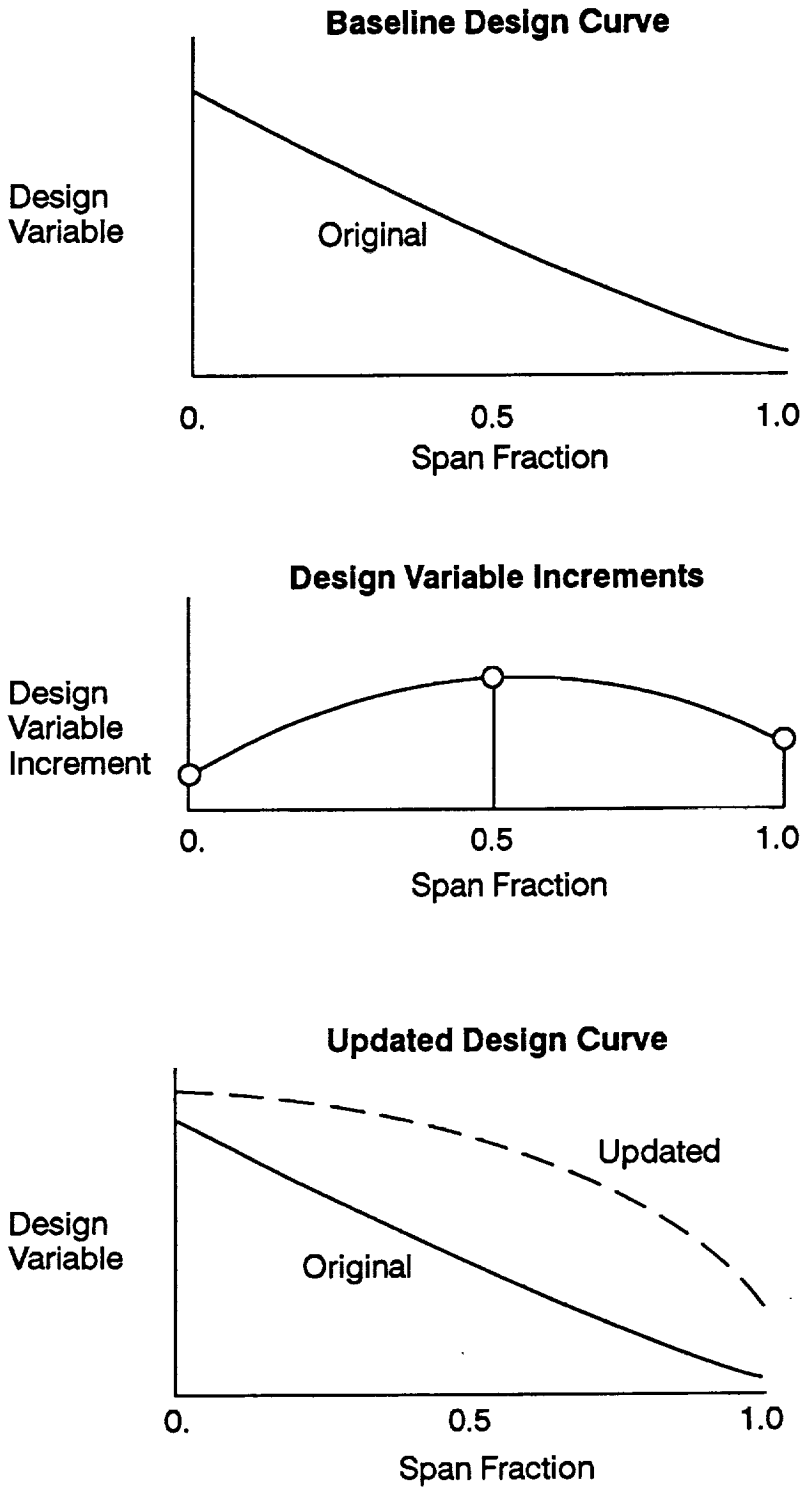

Figure 2. Splined Design Variables from Curve of Design Increments Which Update the Baseline Design

2.2 STAT Optimization Procedure

To provide for increased optimization flexibility and increased program modularity, the ADS optimizer (Reference 2) has been included within the STAT system. ADS is a general purpose numerical optimization program containing a wide variety of optimization algorithms. The solution of the optimization problem has been divided into three basic levels by ADS: (1) Strategy, (2) Optimizer, and (3) One-dimensional search. By allowing the users to select their own strategy, optimizer, and one-dimensional search procedure, considerable flexibility is provided for finding an optimization algorithm which works well for the specific design problem being solved.

Within STAT, the optimization algorithm is selected through the OPTIMIZE data card, which allows for input of the ISTRAT, IOPT, ISERCH, and IOUT parameters. These parameters are used to select the strategy, optimizer, one-dimensional search, and output algorithms as described below.

For the STAT application, 0 5 8 has proven to be the most reliable method for constrained optimizations using equality and inequality constraints (the SR7, 18E, and CRPX test cases), while 0 3 3 has proven to be the best procedure for the unconstrained optimization of aeroelastic scale models. The optimizer output selection used for all of STAT's applications has been 3552 to date.

Strategy

The optimization strategies available in STAT are listed in Table 1. The parameter ISTRAT is sent to the ADS program to identify the strategy selected by the user. Selecting the ISTRAT=0 option transfers control directly to the optimizer. This is selected when choosing the Method of Feasible Directions or the Modified Method of Feasible Directions for solving the constrained optimization problem.

Table 1 Strategy Options

ISTRAT	Strategy to be Used
0	*None. Go directly to the optimizer.*
1	*Sequential unconstrained minimization using the exterior penalty function method.*
2	*Sequential unconstrained minimization using the linear extended interior penalty function method.*
3	*Sequential unconstrained minimization using the quadratic extended interior penalty function method.*
4	*Sequential unconstrained minimization using the cubic extended interior penalty function method.*
5	*Augmented Lagrange Multiplier Method.*
6	*Sequential Linear Programming.*
7	*Method of Centers.*
8	*Sequential Quadratic Programming.*
9	*Sequential Convex Programming.*

Optimizer

The IOPT parameter selects the optimizer to be used by ADS. Table 2 lists the optimizers available within STAT. Note that not all optimizers are available for all strategies. Allowable combinations are shown on Table 4.

Table 2 Optimizer Options

IOPT	Optimizer to be Used
1	*Fletcher–Reeves algorithm for unconstrained minimization.*
2	*Davidon–Fletcher–Powell (DFP) variable metric method for unconstrained minimization.*
3	*Broydon–Fletcher–Goldfarb–Shanno (BFGS) variable metric method for unconstrained minimization.*
4	*Method of Feasible Directions for constrained minimization.*
5	*Modified Method of Feasible Directions for constrained minimization.*

One–Dimensional Search

Table 3 lists the one–dimensional search options available for unconstrained and constrained optimization problems. The parameter ISERCH selects the search algorithm to be used.

Table 3 One–Dimensional Search Options

ISERCH	One–Dimensional Search Option
1	*Find the minimum of an unconstrained function using the Golden Section method.*
2	*Find the minimum of an unconstrained function using the Golden Section method followed by polynomial interpolation.*
3	*Find the minimum of an unconstrained function by first finding bounds and then using polynomial interpolation.*
4	*Find the minimum of an unconstrained function by polynomial interpolation/ extrapolation without first finding bounds on the solution.*
5	*Find the minimum of a constrained function using the Golden Section method.*
6	*Find the minimum of a constrained function using the Golden Section method followed by polynomial interpolation.*
7	*Find the minimum of a constrained function by first finding bounds and then using polynomial interpolation.*
8	*Find the minimum of a constrained function by polynomial interpolation/extrapolation without first finding bounds on the solution.*

Allowable Combinations of Algorithms

Not all combinations of strategy, optimizer, and one–dimensional search are meaningful. For example, it is not meaningful to use a constrained one–dimensional search when minimizing unconstrained functions. Table 4 identifies those combinations of algorithms which are meaningful in the STAT program. In this table, an X is used to denote an acceptable combination of strategy, optimizer, and one–dimensional search, while an O indicates an unacceptable choice of algorithm. To use the table, start by selecting a strategy. Read across to determine the admissible optimizers for that strategy. Then, read down to determine the acceptable one–dimensional search procedures. From the table, it is clear that a large number of possible combinations of algorithms are available.

Table 4 Program Options

			Optimizer		
Strategy	*1*	*2*	*3*	*4*	*5*
0	X	X	X	X	X
1	X	X	X	O	O
2	X	X	X	O	O
3	X	X	X	O	O
4	X	X	X	O	O
5	X	X	X	O	O
6	O	O	O	X	X
7	O	O	O	X	X
8	O	O	O	X	X
9	O	O	O	X	X
One–Dimensional Search					
1	X	X	X	O	O
2	X	X	X	O	O
3	X	X	X	O	O
4	X	X	X	O	O
5	O	O	O	X	X
6	O	O	O	X	X
7	O	O	O	X	X
8	O	O	O	X	X

Optimizer Output Control

The ADS optimizer output is controlled in STAT by the IOUT parameter. This parameter is a four–digit control, IOUT=IJKL where I, J, K, and L have the following definitions:

I: ADS system print control.
- 0 – No print.
- 1 – Print initial and final information.
- 2 – Same as 1 plus parameter values and storage needs.
- 3 – Same as 2 plus scaling information calculated by ADS.

J: Strategy print control.
- 0 – No print.
- 1 – Print initial and final optimization information.
- 2 – Same as 1 plus OBJ and X at each iteration.
- 3 – Same as 2 plus G at each iteration.
- 4 – Same as 3 plus intermediate information.
- 5 – Same as 4 plus gradients of constraints.

K: Optimizer print control.
- 0 – No print.
- 1 – Print initial and final optimization information.
- 2 – Same as 1 plus OBJ and X at each iteration.
- 3 – Same as 2 plus constraints at each iteration.
- 4 – Same as 3 plus intermediate optimization and one–dimensional search information.
- 5 – Same as 4 plus gradients of constraints.

L: One–dimensional search print control.
- 0 – No print.
- 1 – One–dimensional search debug information.
- 2 – More of the same.

Example: IOUT = 3120 corresponds to I=3, J=1, K=2, and L=0.

2.3 Design Variable Scaling

Vanderplaats (Reference 1) has shown that by effective scaling of design parameters, slow or nonconverging optimizations can become quite solvable. This is accomplished by transforming the design variable vector such that all components of the gradient are the same, and the order of magnitude of the components of the diagonals of the Hessian matrix are the same.

To achieve this level of normalization in STAT is likely not possible. However, significant improvements have been noted by normalizing each design variable (dividing by its initial value). This scaling procedure has the effect of putting each variable on the same basis in the sense that a one percent design variable change has roughly the same meaning for each variable. Indeed, this scaling algorithm is built into the ADS optimizer.

In STAT, however, since each design variable represents an updated value from a baseline, the initial value for many or most of the design variables is zero. As such, the built–in scaling of ADS

is rendered useless (the program, to prevent division by zero, simply does not scale a variable whose initial value is zero).

Design variable normalization such as discussed above has been implemented in STAT by normalizing each design variable with respect to its full initial value, as determined from the baseline curves, incremented by the initial design variable increment, if nonzero. This process has been implemented within STAT, external to the ADS optimizer. This can be accomplished within STAT, but not within ADS, since STAT has access to the original, baseline design curves, while ADS does not.

2.4 User–friendly Features

To simplify usage of the STAT program and reduce the chances for errors in creating optimization cases, many user–friendly enhancements have been added to the STAT system. Input cards (Reference 3) are identified by mnemonic titles, and free format inputs are utilized, thus streamlining the data file creation process. Design definition parameters are input as sets of data on CURVE cards, which reference an ABSCISSA card which provides section geometry location. Independent design variables are identified on VARIABLE cards, which provide curve and abscissa value reference for a design variation location. Design variable upper and lower change limits, and initial values for the design variable are also provided. This capability for an initial nonzero value of the design variable provides the program with a restart capability. Associated with the design variables, and providing additional curve perturbation information, are the DEPENDent variables and the CONSTANT terms, which allow curve values at specified locations to be kept constant or to be varied in fixed proportion to variations at design variable locations. Note, CONSTANT cards allow for a restart capability for curves that the user no longer wishes to be varied. This allows the user the freedom to optimize a blade geometry for one particular set of variables and then start with that optimum design and allow STAT to find a new optimum for a second set of variables and soon. These added curve options provide increased program flexibility, and more detailed design curve description, at no additional analysis cost.

3. STAT ANALYSIS MODULES

To perform its propfan optimizations, STAT must be able to evaluate all performance, acoustic, durability, and cost issues for any candidate design. To meet this need, STAT has been given a full set of production quality propfan analysis modules, and is able to fully evaluate the performance characteristics of any conventional or counter-rotating propfan design.

In performing a propfan optimization, as detailed in Section 2, iterative search procedures are employed. Thus, many design iterations, with a corresponding high number of propfan analyses, will be required. To achieve a candidate optimum design as quickly as possible, STAT uses production quality analyses, but employs relatively coarse integration maps. As such, candidate designs may be evaluated as quickly and cheaply as possible, while maintaining acceptable levels of analysis accuracy. An optimal design can easily be analyzed in more detail simply by using a more detailed integration network (computer memory permitting).

Should one of the STAT integration networks prove inadequate for optimization screening, two methods of improving the analysis results are available. First, calibration factors are available in the STAT input stream (see Reference 3) to allow analysis results improvement, at no increase in computer expense. Second, a more detailed mesh may be employed to improve the accuracy of the STAT analysis, though at increased computer cost. Usage of this second procedure may be limited depending on the computer system being used, if sufficient extra memory is not available. For more details on the STAT storage allocation procedure, see Reference 4.

Running Position Geometry Correction

Traditionally, aerodynamic design files define the geometry of the blade in its hot, or running, position because the aerodynamic analysis calculations are strictly dependent upon the running position of the blade. For highly swept fan blades, it is usually left to the structural analyst to define the manufactured, or cold blade geometry such that at running conditions, including gas, centrifugal, and thermal loads, the blade will deflect to the desired geometric position set forth by the aerodynamics group. This is a nonlinear, iterative analysis process and can be quite time consuming.

Using the standard design process, then, the propfan structural considerations trail the aerodynamic design considerations. Indeed, a desirable aerodynamic configuration may not be manufacturable. STAT attempts to assimilate all analysis procedures on an equal, early stage in the design process, to improve inter-disciplinary communications. Thus, STAT is really a concurrent design analysis and optimization process.

Analysis concurrence has been built into STAT by requiring the airfoil design curves to define the cold, as manufactured, airfoil, rather than the hot, running geometry, as is normally done. Within STAT, a module has been added to update an airfoil's cold design by the structural (finite element) deflections, to generate a hot, running position configuration for further aerodynamic and acoustic analysis. There is, however, a bit of a catch to this. After all, how can the hot geometry be calculated if air loads are not known? But, to get the air loads, don't we require a hot geometry?

STAT solves this apparent impasse by recognizing that:

1. Air loads will change little between design iterations

2. STAT is by its nature an iterative process, so initial small errors in air loads will be corrected as the optimum design evolves.

STAT initiates its blade optimization process by performing an aerodynamic analysis of the cold airfoil geometry. Air loads from this analysis are then passed into the optimization loop, which initiates with a finite element analysis, to determine the airfoil hot geometry. As the loop proceeds, each geometry uses the air loads from the previous aerodynamic analysis. Thus, only the first analysis pass uses cold geometry air loads. Each subsequent analysis pass uses hot, nearly correct air loads.

Since the STAT procedure makes smaller and smaller design changes as the optimization proceeds, the differences between the gas loads from one loop to the next will converge to zero and, therefore, the geometry update approximation will become exact. As a byproduct of this airfoil geometry definition convention, when the optimization has been completed, both cold and hot blade geometries are available.

The STAT analysis modules will now be discussed individually, in the order that they are referenced within the optimization loop.

3.1 Airfoil Geometry Generation

For its airfoils, STAT uses standard airfoil definitions, including circular arc, NACA Series 16, NACA Series 62–65, and NACA Series 230. These airfoil shapes, together with the thickness, chord, camber, twist, and stacking design curves, are sufficient to define a unique solid geometry.

For its finite element analysis, STAT employs plate element technology. Thus, to generate the geometry for the airfoil structural analysis, at the finite element mesh points, the coordinates of the foil meanline, as well as the airfoil thickness at those points, will be required.

The airfoil type is selected by the user in the input file, on the GEOMGEN card. The geometry of each radial cross–section is scaled depending on blade thickness and chord. The suction and pressure surfaces of the blade are determined by splining several radial sections from the blade root to tip. Using the surface definitions, the meanline coordinates and thicknesses are calculated for each airfoil gridpoint location.

User alterations to the mesh density to be generated can be accomplished through the STAT input cards, SPANTAB and CHORDTAB. These cards directly supply the program with the fractional chord and fractional span locations of the airfoil mesh gridpoints.

3.2 Finite Element Mesh Generation

STAT's propfan finite element model consists of: (1) the airfoil geometry generated by the geometry generator, (2) effective laminated composite material properties for each airfoil element, and (3) the propfan attachment and hub section.

3.2.1 Plate Airfoil Geometry

Using the array of nodal point locations and thicknesses generated by the geometry generator, creation of a triangular plate mesh of the propfan airfoil is a simple matter. Two options are available:

generate NASTRAN compatible GRID, CTRIA, and PSHELL cards, or, to decrease both computer time and I/O, direct load the geometry into arrays compatible with later geometry processing. Usually, the latter is preferred, but the former is useful for external finite element analysis verification.

3.2.2 Equivalent Properties Generation

Equivalent properties for composite materials are generated in the mesh preprocessor, by applying lamination theory to the composite blade construction while maintaining the blade aerodynamic profile. The layup is treated as symmetric so that no coupling exists between the bending and membrane stiffnesses. Application of lamination theory (Reference 5) to the composite element yields effective stiffness arrays for membrane and for bending motions. These matrices are compatible with NASTRAN material descriptions for the plate elements employed.

When processing material properties of a composite blade for optimization, care is required to ensure meaningful design variable gradients. Due to the high degree of flexibility allowed to the optimizer to move composite plies and hollow cavities, it is not practical to align element edges with ply boundaries. Even if this was accomplished for the initial design, subsequent design perturbations could result in poorly shaped finite elements, which would degrade the accuracy of the approximate finite element analysis.

Within STAT, the element locations and breakup are held constant, and the plies are allowed to shift relative to the element mesh. If an element is fully penetrated by a ply, it is treated as a component of the element in the lamination equivalent property generation. If an element is only partially penetrated by a component ply, the ply thickness is scaled by the area penetration ratio, and a full (but adjusted thickness) penetration is assumed. This algorithm prevents on/off property discontinuities from occurring, and ensures continuous derivatives for the design sensitivity calculations. Note that this algorithm calculates the effective properties for a rectangular "element." Since STAT actually uses triangular finite elements, the properties for one of these rectangular maps is applied to a pair of triangular elements.

Mapping of composite plies onto the finite element mesh is accomplished within STAT through application of design curves to ply shape definition. Composite ply thickness, chordwise extent, and meanline location are defined via design curves. Ply radial extents are defined via cutoff parameters. Each of these ply definition quantities may be treated as a design variable, thus providing much freedom to the composite construction definition. The order of ply layup is defined via the LAYUP card. A PRIORITY card defines which plies will remain in thin sections of the blade, and which plies will be removed. Material directional moduli and Poisson ratios, input on the MATERIAL card, are used to generate equivalent laminar stiffness properties.

The composite ply angle, defined on the MATERIAL card, is used to orient directional composite properties. A ply with zero material angle would be oriented such that its primary axis (1−1 direction) lined up with the projection of the engine radial axis onto the plane of the finite element. Near the tip of these highly swept blades, for the relatively coarse triangular meshes employed for the STAT optimizations, high sensitivity to the calculation of the angle between the element X axis and the projection of the radial axis has been noted. In particular, near the blade tip, the sides (element x−axes) of the quadrilateral elements used to map the composite material properties may not be parallel. To account for this effect, which has a significant effect on airfoil frequency, the element composite ply angle is calculated for each element individually.

3.2.3 Attachment Model

The STAT attachment model can either be defined using NASTRAN bulk data type input cards or directly by defining attachment length and diameter. For highly swept, propfan blades of spar–shell composite structure, the attachment is an extension of the spar and may usually be approximated as cylindrical and therefore, defining the length and diameter is adequate.

The attachment length and diameter may be used as variables. The blade attachment flexibility greatly influences blade resonances; therefore, for frequency tuning, the length and diameter parameters are pertinent variables.

3.3 Finite Element Analysis

The STAT finite element analysis uses NASTRAN's finite element plate technology so as to accurately represent the blade geometry for a large deflection, geometric nonlinear analysis. The plate element more accurately models blade effects such as uncamber and chordwise deflections when compared with beam models. It has been demonstrated with linear finite element analyses that relatively coarse plate meshes yield improved approximate analysis results at run times competitive with beam analysis procedures. Because the STAT approximate analyses must be self–contained, NASTRAN was not a viable approximate analysis option. Hence, a self–contained finite element analysis using NASTRAN plate element technology was constructed.

To enable the application of plate finite element technology to STAT approximate analysis, an efficient plate finite element procedure was created. The procedure uses NASTRAN technology, but because of its reduced scale, all matrices are stored in the core of the computer, and all procedures take place in core as well. Thus, for the small problems of the STAT approximate analyses, the special finite element computer code is able to deliver NASTRAN accuracy, but at greatly reduced computer expense.

3.3.1 The STAT Plate Element

The similarity with NASTRAN was preserved through the usage of a plate bending triangle very similar to the NASTRAN TRIA3 element. The TRIA3 element is a reduced integration triangular plate bending element of the QUAD4 family (Reference 6).

Features of the element include:

1. Recognition of thickness taper
2. Properly stacked triangular plate element meshes to simulate airfoil pretwist and camber
3. Composite material capabilities (using lamination theory)
4. Element differential stiffness
5. Lumped masses are employed, assuring a diagonal stiffness matrix, for storage efficiency.

3.3.2 Guyan Reduction

The Guyan reduction procedure (Reference 7) has proven to be a very successful means of reducing the number of degrees of freedom used in dynamic analysis, while minimizing loss of accuracy in the lower frequency modes. The procedure is based on the fact that many fewer grid points are needed to describe the inertia of a structure than are required to describe its stiffness with comparable accuracy. The reduction procedure thus allows a condensation, resulting in a much smaller equation set for dynamic analysis.

The reduced, or omitted, degrees of freedom, Uo, and the remaining, or analysis degrees of freedom, Ua, relate to static loads according to:

$$\begin{bmatrix} Kaa & Kao \\ Koa & Koo \end{bmatrix} \begin{Bmatrix} Ua \\ Uo \end{Bmatrix} = \begin{Bmatrix} Fa \\ Fo \end{Bmatrix} \tag{1}$$

Neglecting the forces Fo, we find;

$$\{Uo\} = [Goa]\{Ua\} \tag{2}$$

where

$$[Goa] = -[Koo]^{-1}\,[Koa] \tag{3}$$

The matrix decomposition required to calculate Goa in Equation (3) was accomplished by using the LEQ1PB subroutine of the International Mathematics and Statistics Library (IMSL).

The reduced stiffness matrix thus becomes:

$$[Kaa] = [Kaa] + [Kao]\,[Goa] \tag{4}$$

The reduced mass matrix, determined by equating the kinetic energies before and after the reduction, is:

$$[Maa] = [Maa] + [Mao]\,[Goa] + [Goa]^{T}\,([Moa] + [Moo]\,[Goa]) \tag{5}$$

3.3.3 Differential Stiffness

The determination of natural frequencies for rotating blades requires the inclusion of differential stiffness effects due to centrifugally induced steady stresses. In order to allow for differential stiffness generation, static deflections are determined for the case of centrifugal loadings, using the LEQT1P solver of the IMSL package. The static displacements are then used to create the element differential stiffness matrix, KDGG. The energy of differential stiffness, Ud, consists in part of energy of bending motions, Udb, and in part of membrane (in−plane) motions, Udm:

$$Ud = Udb + Udm \tag{6}$$

As shown in Reference 8, the bending and membrane energies are related to the membrane stresses and the bending rotations, giving an energy per unit area of:

$$U' = \frac{h}{2}\left\{\bar{\sigma}_x(\omega_y)^2 + \bar{\sigma}_y(\omega_x)^2 - 2\bar{\tau}_{xy}\omega_x\omega_y\right\} +$$

$$\frac{h}{2}\left\{\bar{\sigma}_x(\omega_z^2 + 2\omega_z\varepsilon_{xy}) + \bar{\sigma}_y(\omega_z^2 - 2\omega_z\varepsilon_{xy}) + 2\bar{\tau}_{xy}(\varepsilon_y - \varepsilon_x)\omega_z\right\} \tag{7}$$

where h is the element thickness; $\bar{\sigma}_x$, $\bar{\sigma}_y$, and $\bar{\tau}_{xy}$ are the element membrane stresses; and ω_x, ω_y, and ω_z are the rotations in the element coordinate system, shown on Figure 3.

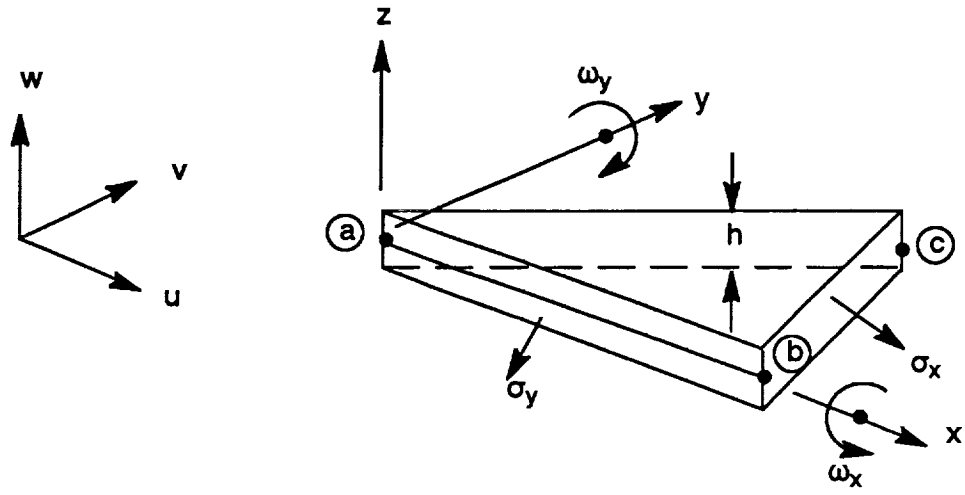

Figure 3. Stresses and Rotations of Prestress Stiffened Plate Element

The centrifugal mass matrix, which accounts for the change in direction of centrifugal loads with displacement, gives the nodal incremental load in global coordinates (x = radial, z = axial), as:

$$\begin{Bmatrix} Fx \\ Fy \\ Fz \end{Bmatrix} = \begin{bmatrix} M\Omega^2 & 0 & 0 \\ 0 & M\Omega^2 & 0 \\ 0 & 0 & M\Omega^2 \end{bmatrix} \begin{Bmatrix} X \\ Y \\ Z \end{Bmatrix} \tag{8}$$

This "stiffness," transformed into local nodal coordinates, is combined with the differential stiffness matrix and the original blade stiffness, to give the blade's total at–speed stiffness. The total blade stiffness matrix, after reduction to analysis–set size, is solved to find the at–speed blade natural frequencies.

3.3.4 Eigenvalue Solution

Once the stiffness and mass matrices have been reduced, they are, in general, symmetric but full. Due to the reduction procedure, however, they are relatively small in size. The unsymmetric eigenvalue problem is formed:

$$-\omega^2\{Ua\} + [Maa]^{-1}[Kaa]\{Ua\} = \{0\} \tag{9}$$

The IMSL subroutine package is again employed, using the QR method to solve the unsymmetric eigenvalue problem. Both eigenvalues and eigenvectors are extracted for the reduced size problem. IMSL routines required to perform the eigenvalue extraction include: EBALF, EHESSF, EHBCKF, EQRH3F, AND EBBCKF.

3.3.5 In–Plane Rotation Singularity Constraint

When performing plate finite element analysis, the in–plane rotations must be suppressed in relatively flat sections to prevent system ill–conditioning. On airfoils, camber is usually sufficient near the blade root to prevent in–plane rotation singularities. Near the blade tip, however, camber is low and suppressions are usually required. In large deflection analyses, the problem is further compounded by the possibility that the blade section may uncamber during the deflection process, thus introducing further singularities.

To prevent against possible numerical problems during the STAT analyses, an algorithm to provide an artificial stiffness to in–plane rotation singularities has been included in the STAT finite element code. The algorithm, taken from Reference 9, creates a fictitious set of rotation stiffness coefficients that is used in all elements, whether co–planar or not. For the triangular plate element, the stiffness is defined by a matrix such that in element local coordinates, equilibrium is not disturbed, namely:

$$\begin{Bmatrix} Mz1 \\ Mz2 \\ Mz3 \end{Bmatrix} = \alpha EtA \begin{bmatrix} 1. & -.5 & -.5 \\ -.5 & 1. & -.5 \\ -.5 & -.5 & 1. \end{bmatrix} \begin{Bmatrix} z1 \\ z2 \\ z3 \end{Bmatrix} \tag{10}$$

where the coefficient was found through numerical tests to provide numerical stability with negligible artificial system constraint for a value of $\alpha = 1.x10-6$.

3.3.6 Geometric Nonlinear Analysis

The geometric nonlinear finite element analysis in STAT permits analysis of structures which undergo large deflections and rotations. Material linearity is maintained by requiring that the strains in any finite element remain small. In a linear static analysis, all coordinate systems are assumed to be stationary with respect to an inertial frame. The nonlinear static analysis permits the local element coordinate system to translate and rotate relative to the reference frame. Whereas this coordinate system motion may be large, the relative element deflections must remain small. The relative element deflections are obtained through coordinate transformations. It is these transformations which introduce the geometric nonlinear relations.

The Geometric Nonlinear Analysis:

The linear static analysis, a two step process, precedes the nonlinear solution. Step one of the linear static analysis includes assembling the structure stiffness, K, and external loads, P. Deflections, U1, are obtained through the product of the stiffness matrix inverse and the external load vector.

$$(U1) = [K]^{-1} (P) \tag{11}$$

Step two utilizes these deflections to produce a linear correction on the initial stiffness to account for the effect of load, deflection interaction. This correction is called the differential stiffness, Kd, and is used to modify the original stiffness, K. The second solution is obtained;

$$(U2) = [K + Kd]^{-1} (P) \tag{12}$$

The nonlinear solution process is simply an extension of the linear static procedure, and in fact builds on the linear static solution, U2. In simplest terms, the nonlinear solution involves an iterative process which converges when the external and internal loads are in equilibrium. The iteration process uses the previous solution vector to form an incremental element stiffness matrix and internal force vector. The incremental stiffness is combined with the initial stiffness similar to the differential stiffness procedure. Internal forces are then calculated from the product of the modified stiffness and the deflections. New external loads may be regenerated based upon the deflected shape. The difference of the external and internal load vectors multplied by the inverse of the modified stiffness produces an incremental deflection vector. The incremental deflection vector magnitude approaches zero as the force equilibrium is achieved. The nonlinear iteration process is discussed in greater detail below.

The nonlinear iteration process begins with the formation of three transformation matrices:

[Teb] – basic system to undeformed element system,

[Tdb] – basic system to deformed element system,

[Tbg] – basic system to local grid (or global) system.

The basic system refers to the stationary reference coordinate system. These matrices are used to transform the global (nodal referenced) deflections, Ug, to the deformed element system producing the relative deflections, Ud, at node i;

$$(Ud_i) = [Tdb]\left((X_i) + [Tbg_i]\,(Ug_i) - (Rd) \right) - [Teb] * \left((X_i) - (Re) \right) \qquad (13)$$

where: X – undeformed coordinate
Re – undeformed position vector
Rd – deformed position vector.

Relative rotations require a different procedure because finite rotations do not add vectorially. Instead, the rotations are performed sequentially, first about global z, then about the reoriented y, and finally about the twice reoriented x. The resulting rotation operations when combined form the rotation matrix, R(Og);

$$R(\theta g_i) = \begin{bmatrix} CzCy & CzSxSy - SzCx & CxCzSy + SxSy \\ CySz & SxSySz + CxCz & CxSySz - CzSx \\ -Sy & CySx & CxCy \end{bmatrix} \qquad (14)$$

where; Cx = cos (Rx) ; Sx = sin (Rx)
Cy = cos (Ry) ; Sy = sin (Ry)
Cz = cos (Rz) ; Sz = sin (Rz)
i = loop thru all nodes on element

and Rx,Ry,Rz are global rotation components at node i.

This matrix is then transformed to produce the relative element rotations, R(θd), at node i;

$$R(\theta d)_i = [Tbd]^T\,[Tbg_i]\,[R(\theta g)_i]\,[Tbg_i]^T\,[Teb] \qquad (15)$$

Because rotations within the element are small R(θd) may be written;

$$R(\theta d)_i = \begin{bmatrix} 1 & \theta z & -\theta y \\ \theta z & 1 & \theta x \\ \theta y & -\theta x & 1 \end{bmatrix} \tag{16}$$

where θx, θy and θz are the relative element rotations at node i.

The element incremental stiffness, Kde, is determined knowing the relative deflections and rotations, and then added to the original element stiffness, Ke. Local element internal forces, Fi, follow:

$$(Fi) = [Ke + Kde]\ (Ud) \tag{17}$$

The updated element stiffness and the internal force vector are assembled to the global level. The assembled internal vector is subtracted from the external load vector, P, forming the incremental load vector, L. Incremental deflections are directly solved;

$$(U)_j = [Kg]\ (L)_j \ , \ j = \textit{iteration counter}. \tag{18}$$

The incremental translations may be added directly to the previous solution total deflection vector, U(j−1), forming the current deflection vector, U(j);

$$U(j) = U(j-1) + U(j) \tag{19}$$

The incremental rotations are added to the total rotations via the following;

$$\begin{aligned} Rx(j) &= Rx(j-1) + term\ /\ CY \\ Ry(j) &= Ry(j-1) + term \\ Rz(j) &= Rz(j-1) + term\ /\ Cy\ *\ SY + Rz(j) \end{aligned} \tag{20}$$

where; term = Ry(j) * SZ + Rx(j) * CZ
SY = sin(Ry(j−1))
SZ = sin(Rz(j−1))
CY = cos(Ry(j−1))
CZ = cos(Rz(j−1)).

Solution convergence may be determined from U(j) or the change in strain energy. If the solution does not meet the convergence criterion, then the iteration process continues thru another pass. This continues until convergence is achieved or until the maximum allowable number of passes has been completed.

The iteration process may be sped up by not rebuilding the stiffness matrix or the external load vector during each pass. This may result in more iterations being required to achieve a converged solution, but each iteration is faster due to fewer matrix operations. As the problem becomes more nonlinear such "shortcuts" are not advisable. The nonlinear iteration process is successful only if the first solution is relatively close to the converged answer.

Nonlinear Analysis Control Cards:

The nonlinear analysis is controlled through bulk data input cards. These cards define multiple loads and application order, and the regeneration of the stiffness matrix and external load vector. Each of the these cards is preceded by $$PARAM which indicates this card is a control card. The nonlinear analysis is turned on or off through the NONLIN control card. A linear static analysis is the default if no NONLIN control card exists. The load controller is called LOADID. Up to 8 loads may be requested. Each load will be sequentially iterated until convergence is achieved or until MAXITER has been exceeded. The next load is started using the previous load resultant deflection. Load increments which are far apart may not provide sufficiently good initial estimations for the iteration process to converge. The SKPMAT control card permits the user to specify which load cases are to reconstruct the stiffness matrix during each iteration. The SKPLOAD card provides similar control on the external load vector. Regeneration is the automatic default for both SKPMAT and SKPLOAD. Use of the EIGEN card permits eigenvalue calculation for any converge load set. The PRINT control card provides standard NASTRAN printed output for any converged load static and eigenvalue analyses.

Nonlinear Analysis Guidelines:

The major goal of any nonlinear analysis is producing a converged solution in a minimum of computer time. As explained earlier, the iteration process success is dependent upon the starting point it is given. A starting deflection vector which is far from the correct solution will not converge or will converge very slowly. Therefore, the challenge lies in choosing a sequential series of partial loads, each building on the previous, ending with the total load which produces the correct converged solution. A structure which is nearly linear will need only a single load equal to the full load to converge. A more nonlinear structure may require two, three, or more partial loads to achieve a converged solution at the full load.

A poor load choice will be evident from two sources. First, convergence will not be achieved within the MAXITR limits. Experience has shown if convergence is not achieved within 10 passes, the load increment was too large. In such a case, the convergence criterion whether deflection or strain energy based will oscillate and diverge. The second failure mode involves a 'Terminal Error' issued from the program stating that a matrix operation failed due to a stiffness singularity. This indicates the structure has become unstable or is 'buckling,' again indicating that the load increment was too large. As the structure get closer to this buckling limit, the required load increment size will decrease. In fact, some of the more aggressive propfan designs attempted by STAT have failed at part speed loads.

3.3.7 Postprocessing of Finite Element Output

The STAT finite element code provides, as output, static displacements and stresses (for the composite equivalent elements), as well as at–speed eigenvalues, eigenvectors and modal equivalent stresses. Many of these data blocks must be postprocessed before they may be used either for constraint evaluation or as input to other subroutines. Element stresses must be converted to composite ply stresses for the static deformations and natural modes. Blade sectional mass properties must be evaluated from the assembled finite element mass matrix. Additionally, the flutter analysis requires frequency, mode shape, and generalized mass information.

The evaluation of static and modal composite blade ply stress values requires processing of the element stress values based upon the application of lamination theory (Reference 5). The lamination theory assumes that plane sections (through the plate thickness) remain plane after deformation. The

laminate processor provides the matrices required to convert the element equivalent stresses to membrane and bending strains. Then, based on the lamination assumptions, ply strains are calculated, leading to ply stresses, and, ultimately, to the TSAI–WU tensor failure theory equivalent stress evaluation (Reference 10).

The objective function for scale model tailoring requires the blade section mass distribution for comparison with the full blade mass properties. The full sized, assembled finite element mass matrix is used to evaluate the total mass at each radial station of the finite element blade by using a simple averaging scheme. The difference between the inertia properties of the blade and its scaled model are then evaluated.

The evaluation of flutter constraints requires that equivalent beam mode shapes be generated from the available plate mode shape data, due to the beam theory of the present flutter codes. Beam mode shapes are generated from the available plate mode shapes by performing a spline fit of each component of the mode shape on each cross section. From the spline fit, modal bending and torsional motions are determined at the section shear center, for transmittal to the flutter analysis.

3.4 Flutter Stability Analysis

The STAT flutter analysis performs both the unstalled and stalled flutter calculations. Each flutter analysis proceedure is described as follows:

3.4.1 Supersonic Unstalled Flutter Analysis

The unstalled flutter stability subroutine was specifically tailored to model the structural and aerodynamic complexities of the propfan. The blade structure is represented by fully coupled mode shapes. The coupled modes take the form of translation normal to the blade surface at the mid–chord and rotations about the blade mid–chord. The mode shapes are passed to the subroutine from the finite element analysis routines. Unsteady airloads are formulated using strip theory with no induced velocities included. The blade is divided into a series of discrete aerodynamic panels of constant property. Each panel is defined with plunging and pitching about the mid–chord reference specified by the mode shape displacement definition. Unsteady, unstalled lift and moment equations for the two–dimensional panels are generalizations of the unsteady swept aerodynamic equations generated by Barmby, Cunningham, and Garrick in NASA TN 2121. The equations are modified to account for compressibility and sweep. Cascade effects are taken into account in the analysis with an empirical correction based on propfan model tests.

3.4.2 Stalled Flutter Analysis

The stalled flutter stability analysis is based on empirical data used to prevent torsional stall flutter of propeller blades. The blade mode shapes passed to the subroutine are examined to determine the torsion mode. The torsional frequency is then used to calculate a stall flutter parameter that must be greater than one for a given configuration to be free from torsional stall flutter.

3.5 Airfoil Hot Geometry Update

As discussed in Section 3, the airfoils defined in the STAT input stream, and carried throughout the STAT optimization process, are defined in the cold, or as manufactured, geometry. Defining the STAT airfoils in this manner eliminates an iterative, difficult, time–consuming finite element analysis step from the standard design process. In order to accurately determine the aerodynamic efficiency and acoustic emissions of a propfan rotor, however, requires analyses performed for the hot, running airfoil geometry.

To provide a proper description of the running geometry, STAT includes a geometry update module. Working with each rotor stage separately, this module uses the airfoil cold meanline geometry, and updates the geometry by the airfoil deflections obtained from the finite element analysis, to determine the actual running position. Recall that STAT employs the air loads from the previous design iteration. Since the air loads change little from iteration to iteration, the error introduced in this process is quite small, and becomes negligible as the optimization process takes smaller and smaller design changes near the optimized design.

The procedure used by the geometry update module is to use the meanline geometry for the cold blade, and update the positions of the meanline points by the deflections obtained from the finite element stress analysis. This new meanline is then converted back to a standard airfoil section by updating the stacking coordinates, twist angle, and camber of the original airfoil definition. Thus, the standard airfoil section that is closest to the actual running position is determined. This updated airfoil description is then passed to the aerodynamic and acoustic analysis modules, to determine efficiency, acoustic emissions, and updated air loads.

3.6 Aerodynamic Efficiency Analysis

The module used to calculate propeller efficiency is a high–speed propeller–nacelle aerodynamic performance method (Reference 12). The method uses lifting line theory, with a swept bound segmented vortex, and prescribed trailing segmented vortices. The induced velocity from each vortex segment can be expressed, using the Biot–Savart equation, as a function of vortex segment position, field point and the vortex strength. Through a matrix inversion, blade circulation and induced velocity are solved.

The method contains compressible features for blade induction and blade profile losses. The law of forbidden signals corrects the induced velocity when relative Mach numbers are greater than one. The compressible 2–D airfoil data used is also corrected for Mach numbers greater than one by applying a Mach Cone correction (Reference 13).

The same method is used for both the approximate and refined analyses. The difference stems from the number of radial stations used to define the airfoil geometry and aerodynamic flow. The approximate analysis uses 10 radial stations, while 14 radial stations are recommended for refined analyses. Additionally, the analysis is performed on the hot running position of the blade and is therefore called after the finite element analysis has been completed, and a deformed, running geometry has been determined.

For analysis of counter–rotation propfan systems, the rotor systems may have different blade counts front and rear. This results in a loss of symmetry, resulting in a more detailed, much more costly aerodynamic analysis. For STAT's approximate optimization procedure, the assumption has been made that, for determining the system efficiency, two analyses of rotor systems of equal blade count could be used to closely determine the efficiency of a system with unequal blade counts.

Thus, to analyze a rotor system with 10 blades in the front stage and 8 blades in the rear stage, STAT performs two aerodynamic performance analyses. The first analysis is on a 10 X 10 system. The results of this first analysis are used to determine the efficiency of the front stage. The second analysis, on an 8 X 8 system, is used to determine the efficiency of the rear stage. The resulting overall combined efficiency is very close to that obtained from a much more costly, 10 X 8 analysis. Checks performed with a detailed, refined analysis showed this approximation to be very good – the efficiency error was only 0.2 percent, with a significant computer expense savings.

3.7 Acoustic Emissions Analysis

In the propfan design process, two acoustic emissions situations are important: far-field noise and near-field noise. For a propfan design optimization, far-field noise is generally not included. While a propfan must meet the Federal Aviation Regulation (FAR) P-136 noise limit to be certifiable, the far-field noise depends primarily on the major design parameters, such as blade count, tip speed, and power loading. As such, the design variables available to a STAT optimization have little or no effect on the far-field noise, so this acoustic component is not included in the STAT optimization system.

Near-field noise does not directly impact fuel burn, but it does affect aircraft system cost, as high emissions imply an increased weight of fuselage acoustic treatment needed to achieve the required cabin noise level. Thus, increased near-field noise results in increased aircraft weight, and hence, a higher cost aircraft system.

Within STAT, the near-field noise calculation is based on the Hanson frequency-domain propfan noise theory. Sources of near-field noise during high speed cruise include: blade thickness, blade air loading, and nonlinear (quadrupole) effects. Factors that reduce the cabin noise level include fuselage attenuation and wing shielding effects.

The nonlinear quadrupole noise, which is neglected by most calculation procedures, has been found to be important for propfan applications. In fact, it has been found to be the dominant noise effect at the higher harmonics for transonic tip speed conditions. Sweeping the propfan blade, either forward or aft, has been shown to be a powerful method for reducing the near-field noise. This sweep introduces a phase shift along the blade span, which promotes noise cancellation. Of course, introducing blade sweep introduces structural complications such as increased stress, which must be balanced through the STAT optimization process.

To account for the combined emissions effect of a counter-rotating propfan system, STAT calculates the near-field noise of each individual rotor. The total near-field noise is then calculated by using a root sum square method, with a factor included to account for rotor to rotor spacing.

The impact of near-field noise on fuel burn is through the weight of acoustic treatment required to meet the cabin noise goals. Defining the treatment requirements is not trivial, due to the periodic nature of the incident noise, which allows for interaction with the fuselage structural modes, as well as cabin interior acoustic modes. The treatment calculation used by STAT is based on a double limp wall concept developed by the Lockheed-California company. This procedure uses the exterior free-field noise level as its input, and calculates the amount of acoustic treatment weight required to meet cabin noise allowables. This acoustic treatment weight may then be translated to effective fuel burn rates within the objective function module.

3.8 Once-Per-Revolution Forced Response Analysis

Due to the angle between the engine axis and the aircraft forward velocity vector, propfans are subject to a relatively high once-per-revolution (1-P) excitation force. The system vibratory response to this excitation must be calculated to ensure adequate fan durability.

3.8.1 One-P Loads

The propeller 1-P loads are calculated at a user-supplied airplane yaw angle. The method utilizes Goldstein induction theory, Reference 11, and the same compressible 2-D airfoil data used by the aerodynamic module to calculate the advancing and retreating blade peak to peak loads.

The induced velocity is determined from Goldstein induction factors which are functions of local radius, number of blades, and wake pitch. The induction factors are precalculated and tabulated from the Goldstein equations. The wake pitch includes the induced flow, requiring an iteration for solution, but allows the method to be used successfully for most propeller loadings. The module calculates deflected 1−P loads.

For counter−rotating propfan systems, STAT performs the 1−P loading analysis on the first−blade only. Loads for the second blade are generated by applying a load factor to the first blade loads.

3.8.2 Forced Response Calculation

The calculated 1−P loads for the hot running position are used to calculate the modal load for each of the first five blade frequencies. The modal loads are in turn divided by the blade frequency generalized stiffness to define the static deflection due to the 1−P loads. For a given blade frequency i:

$$\begin{aligned} K_i &= M_i * (\omega_i)^2 \quad \text{... generalized stiffness} \\ Us_i &= P_i / K_i \quad \text{... static deflection} \end{aligned} \tag{21}$$

The static response is then amplified depending upon the one−dimensional forced response magnification relationship (Reference 8) as follows;

$$\begin{aligned} R_i &= 1 / \left[1 - \left(\omega_i / \omega_{engine}\right)^2\right] \\ A_i &= Us_i * R_i \quad \text{... modal amplification} \end{aligned} \tag{22}$$

to arrive at the modal participation factors for the first five blade frequencies.

The modal stresses multiplied by their participation factors are summed up for the first five modes to calculate blade vibratory stress in response to the 1−P excitation load. Then the Tsai−Wu layer stresses are processed using the calculated vibratory stresses and along with the Tsai−Wu layer stresses calculated for the steady airloads and rotational force, a life limiting relationship was defined as;

$$TWvs_{n,k} + TWss_{n,k} < 1.0 \tag{23}$$

which implies that the sum of the vibratory and steady Tsai−Wu stresses for the nth layer of the kth element must be less than one in order to avoid HCF failure due to 1−P excitation.

3.9 Objective Function

STAT supports the minimization of two distinct objective functions. The first objective function seeks to maximize propfan performance and minimize operating cost by trading weight, efficiency, and acoustic emissions according to user−input trade factors. Should the user decide to include other performance parameters such as power, sweep, or activity factor, coefficients may be defined for weighting these factors also.

The second STAT objective function attempts to minimize the differences between a propfan rotor system and its aeroelastic scale model, by tuning the scale model to match both static and vibratory performance characteristics. In each case, the final STAT objective function is a summation of the weighting factors times the appropriate performance factors over each stage in the propfan system.

3.9.1 Propfan Performance Objective Function

Factors that determine the operating cost of a propfan rotor system include its aerodynamic performance, its acoustic emissions, and its weight. The cost sensitivity factors, obtained from aircraft or engine companies, vary with aircraft type, size and mission. The factors supplied for the STAT test cases are based on a 120 passenger, 0.8 Mach number, 1200 nautical mile, twin engine aircraft. Generalizations for propeller gearbox weight and acoustic treatment weight are approximations but are included in the DOC (direct operating cost) calculation. The DOC is calculated relative to a user–defined baseline propeller.

At times, DOC is not of primary importance. The user may wish to find a rotor that meets the durability requirements, yet minimizes sweep, for instance. At times, propfan activity factor is an important design criterion. To provide the flexibility for optimizing on these non–cost objective functions, the STAT objective function includes these parameters.

Thus, the STAT objective function is defined as a linear combination of noise, power, activity factor, tip sweep, airfoil weight, and propfan efficiency, where the user supplies the weighting factors. Note – the weighting factor for propfan efficiency will usually be negative, or STAT will seek the fan system that has the minimum efficiency!

3.9.2 Aeroelastic Scale Model Tailoring

The definition of the objective function for the tailoring of an aeroelastic scale model of a turboprop fan blade assumes both the scaled and full blade:

1. Have the same tip speed
2. Experience the identical aerodynamic, environmental conditions
3. Have the identical external geometry shape.

With these assumptions, the objective function is structured so as to minimize the following relationships between the scaled and full blade:

$$(1) \quad \sum_{i=1}^{nmd} \frac{\left[f_{B,i} - k * f_{S,i}\right]^2}{\left[f_{B,i}\right]^2} \quad \text{... blade resonances}$$

$$(2) \quad \sum_{i=1}^{nst} \frac{\left[M_{B,i} - k^3 * M_{S,i}\right]^2}{\left[M_{B,i}\right]^2} \quad \text{... mass distribution}$$

$$(3) \quad \sum_{i=1}^{nmd} \frac{\left[(\theta b/d)_{B,i} - (\theta b/d)_{S,i}\right]^2}{\left[(\theta b/d)_{B,i}\right]^2} \quad \text{... modal deflections}$$

$$(4) \quad \frac{(\phi_B - \phi_S)^2}{\phi_B^2} \quad \text{... static deflection}$$

where: nmd represents the number of modes,
nst represents the number of blade stations,
S represents the scale model,
B represents the full blade,
f is natural blade frequency,
M is blade sectional mass,
θ is blade modal tip torsional deflection,
b is blade tip chord,
d is blade modal tip easywise bending deflection,
ϕ is blade static tip untwist, and
k is the model scale factor.

The objective function is defined as the sum of the quantities (1) thru (4). In the limit, as the objective function approaches zero, the aeroelastic differences between the full blade and its scale model are minimized. How well the tailored blade models the aeroelastic characteristics of the full blade depends on the depth of the comparisons made through the objective function and the accuracy of the analytical tools used by STAT. The tailored scale blade will have similar flutter, resonance, efficiency, acoustic, and static and modal deflection characteristics, but because the internal structure of the blade is varied during the optimization process, stress distribution will not be comparable. Thus, a scaled model optimization will have component material stress limits as perhaps the only constraint for its analysis.

For counter rotation propfan systems, the above function is calculated for each rotor, and the sum used as the system objective function.

4. VALIDATION TEST CASES

The STAT program has successfully demonstrated the potential of design optimization when applied to turbo propfan blades of composite construction. The STAT program has been successfully applied to single rotation and counter rotation propfan rotor designs. In all cases, STAT has been able to improve the existing designs, and in all cases finding feasible designs much more quickly than was possible using conventional, manual design iteration processes.

Additionally, the STAT propfan optimum design system has proven to be capable of constructing aeroelastic scale models of both single rotation and counter rotation propfan rotor designs.

4.1 Single–Rotation Propfan Applications

The tailorings of two turbo single–rotation propfan (SRP) rotors were performed successfully using STAT. For these particular cases, the objective function was defined as the aircraft change in direct operating cost (DOC). The DOC was calculated from input aircraft sensitivity factors, and calculated values of propeller efficiency, aircraft fuselage noise level, and propeller weight all relative to the user–defined baseline performance of the SR7 LAP blade. The sensitivity factors used to weigh the different contributors apply to a 120 passenger, 0.8 Mach number, 1200 nautical mile, twin engine aircraft.

The two large advanced–scaled propfan (LAP) blade designs are directly related to one another. The 18E LAP blade is one of the several preliminary designs (87th of a total of 100 designs) of the project from which the SR7 LAP design evolved. The internal composite construction and material, the physical constraints of stress, flutter, power, and resonances, the aerodynamic environment and the blade attachment definitions were all identical for the two designs. But, the external geometry parameters (such as stacking, thickness, twist) of the blades were uniquely defined.

The third and final SRP validation test case was to develop an aeroelastic scale model representation of the SR7 LAP design. The objective function for this optimization process was given careful thought so that the model developed would take on the identical dynamic and static characteristics of the SR7 design. The objective function calculated differences in blade mass distribution, static tip deflection, modal tip deflections and resonances.

4.1.1 The Infeasible 18E LAP Design

The 18E LAP blade design was a preliminary design of the SR7 which was overly stressed for the once per revolution forced response condition. The blade is of a composite construction incorporating a nickel sheath layer for protection against foreign object damage, a fiberglass outer shell, an internal aluminum spar, and foam used to fill the gaps between the spar and the shell to prevent localized shell buckling. The internal construction of the blade is shown in Figure 4. The external geometry of the blade is defined by eight spanwise distribution curves that include blade stacking, twist, chord, thickness, and other pertinent parameters. Figures 5 through 12 summarize the external definition curves of the 18E blade design.

The 18E design constraints involve blade geometry, resonance margins, static stress, once per revolution force response life fraction, classical flutter Mach number, stall flutter and maintaining required driving power. The STAT 18E constraints are summarized in Table 5.

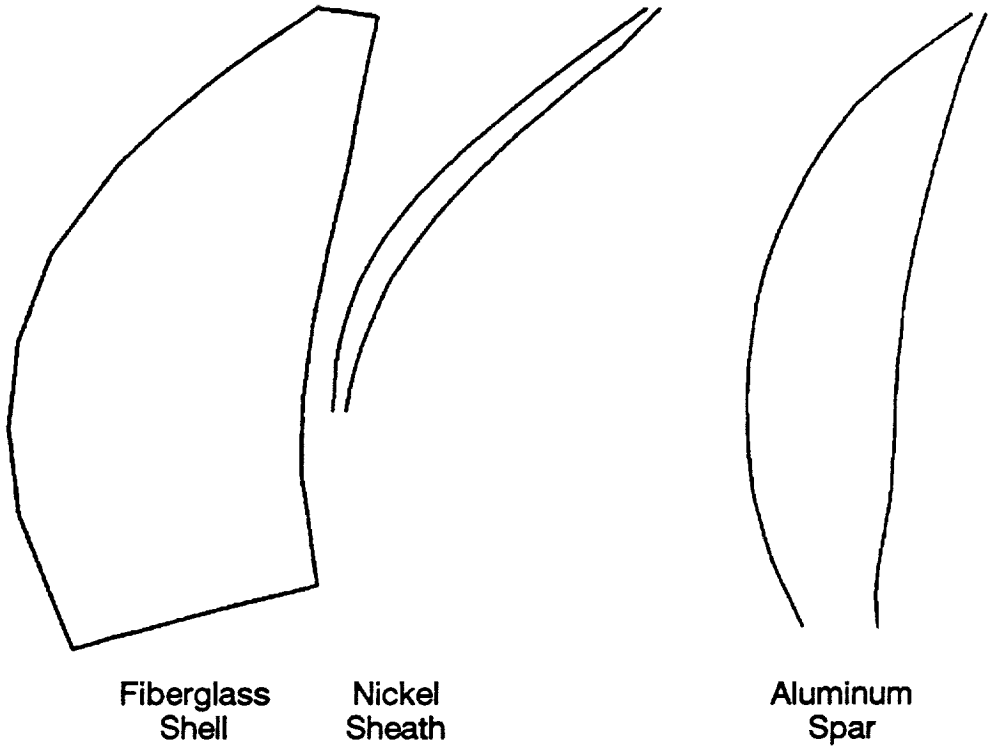

Figure 4. Composite Construction of the 18E Blade

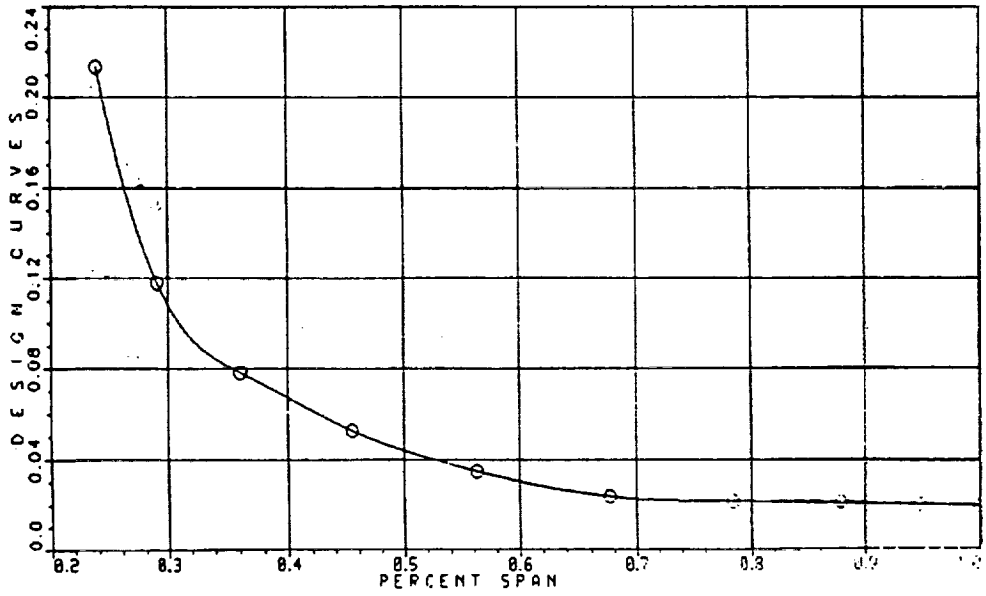

Figure 5. 18E External Curve Definition – Thickness/Chord

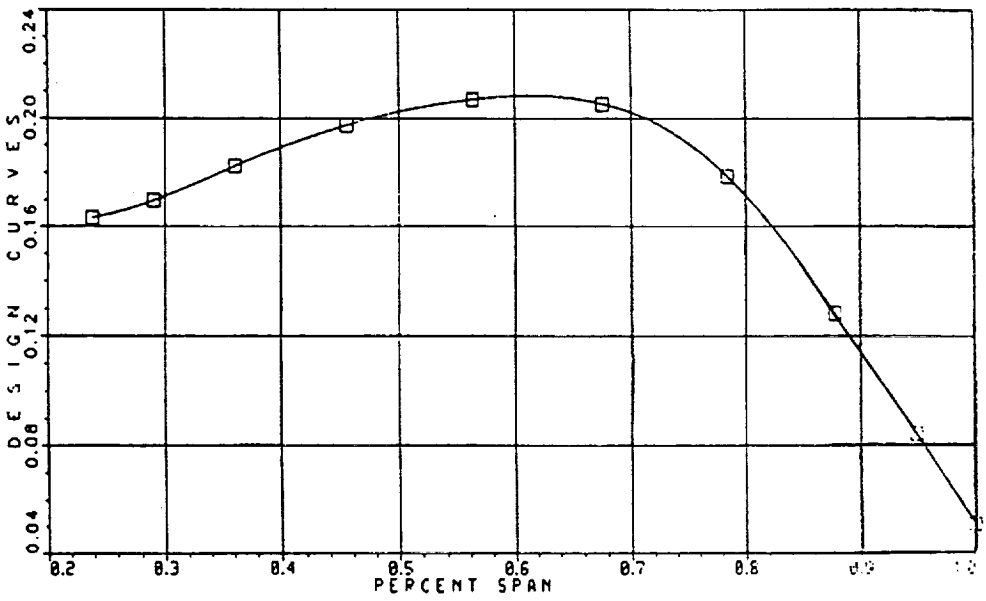

Figure 6. 18E External Curve Definition – Chord/Diameter

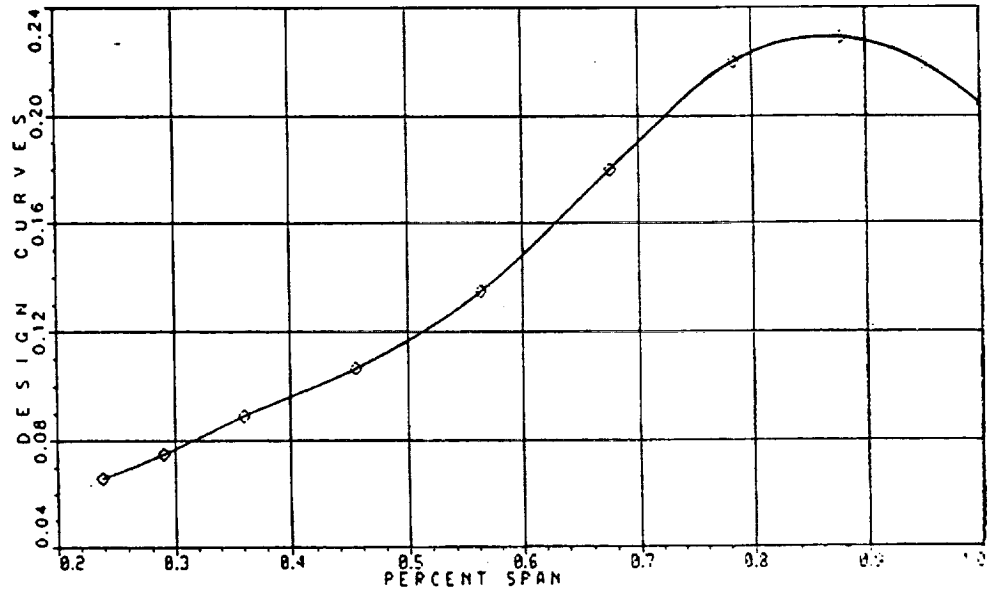

Figure 7. 18E External Curve Definition – Camber/Lift Coefficient

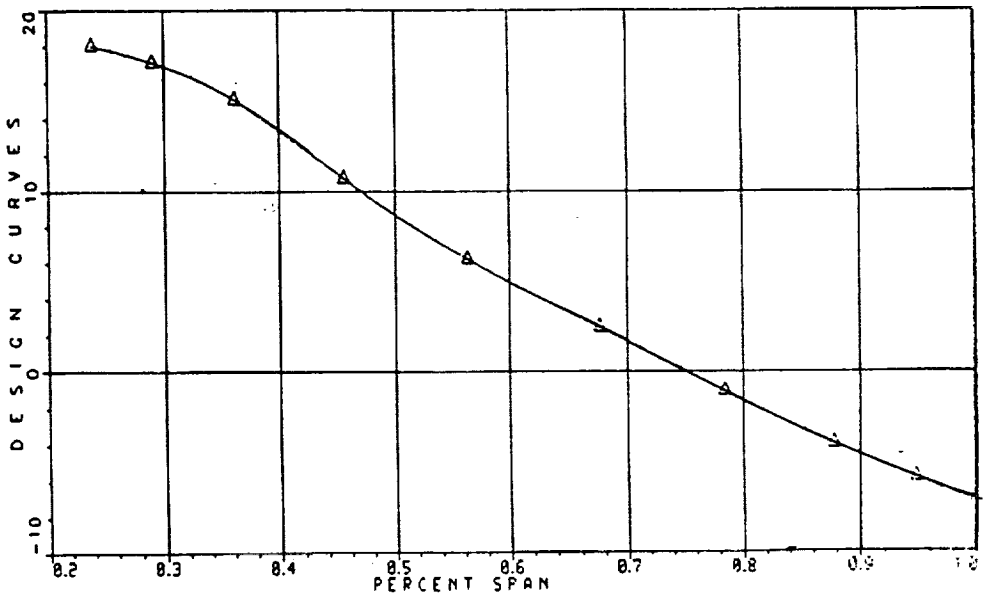

Figure 8. 18E External Curve Definition – Blade Twist

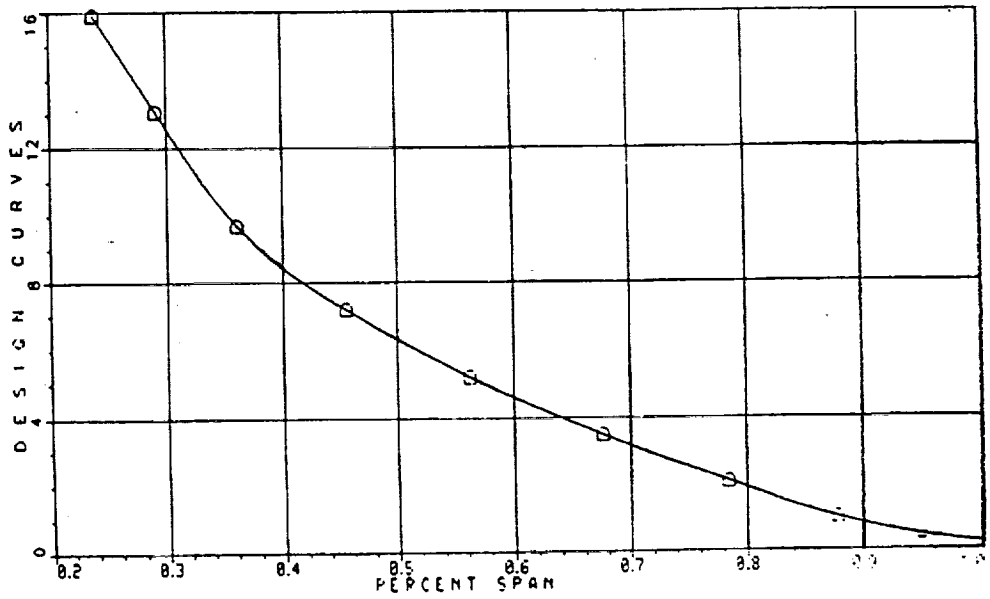

Figure 9. 18E External Curve Definition – Conical Section Angle

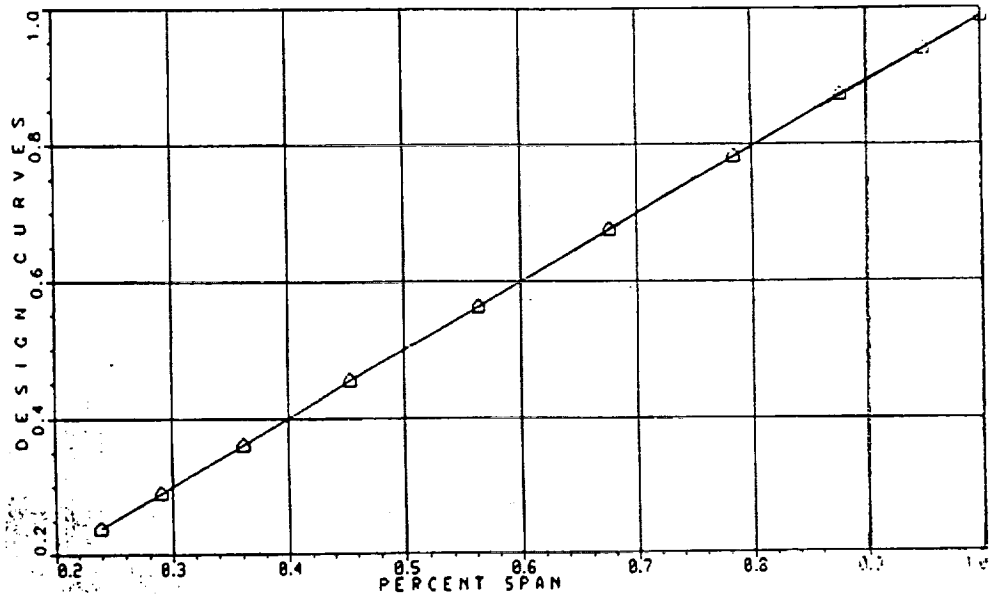

Figure 10. 18E External Curve Definition – Radial Stacking

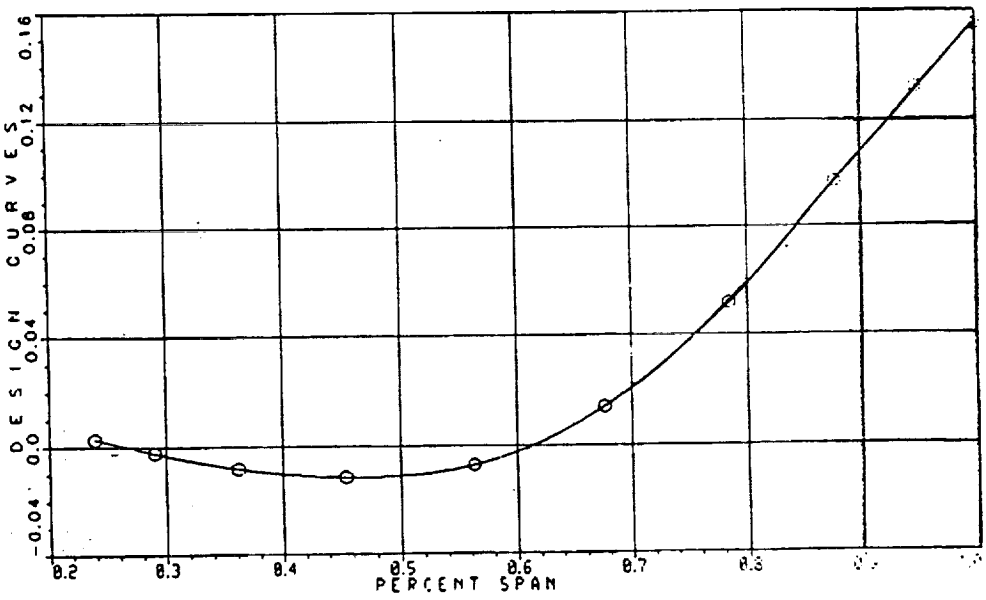

Figure 11. 18E External Curve Definition – Tangential Stacking

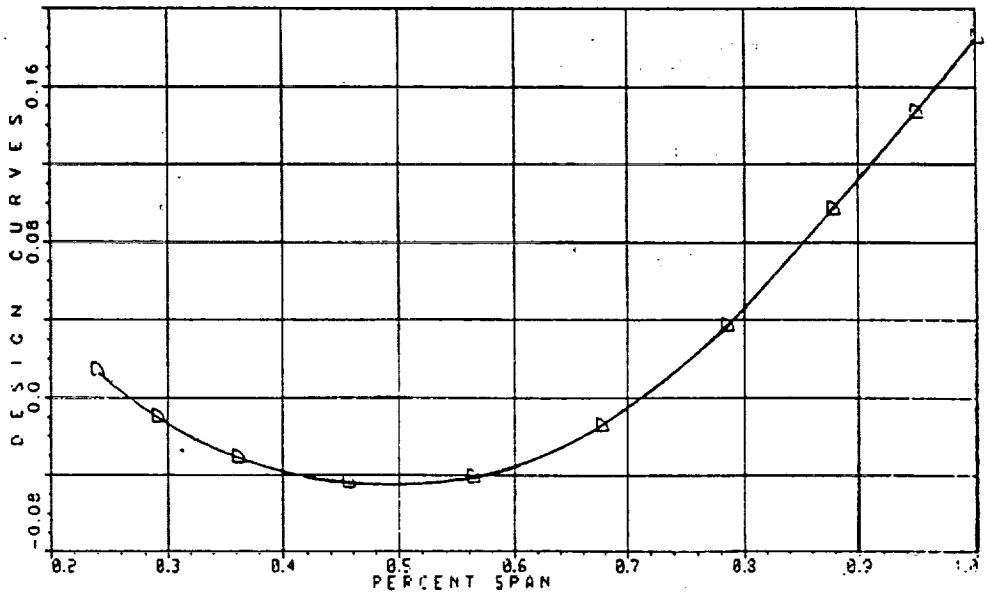

Figure 12. 18E External Curve Definition – Axial Stacking

Table 5 STAT 18E and SR7 Design Constraints

Blade Geometry	*Blade Resonance Margins*
• *Thickness/chord minimums to avoid buckling*	• *1st mode 2E – 10%*
• *Set realistic upper and lower boundaries for all variables*	• *2nd mode 4E – 5%*
• *Maintain root stacking position relative to the attachment*	• *2nd mode 5E – 2.5%*
Blade Flutter	• *3rd mode 5E – 2.5%*
• *Classical flutter Mach number > 0.8*	
• *Stall flutter parameter > 1.0*	*Blade Stress*
Power	• *Tsai–Wu layer steady stress < 1.0*
• *Propfan driving power must be maintained at 2592 hp*	• *Once–per–revolution force response life fraction < 1.0*

The variables used to optimize the 18E design included blade twist, axial stacking and tangential stacking. The stacking variables were used so as to solve the high stress problems, and the twist variables were used to maintain the power required to drive the propeller. The STAT variables and their blade locations are summarized in Table 6.

Table 6 STAT 18E Optimization Results

Design Variables	*Change Limits*		*Opt Update*
Blade Twist			
45.5%	*−90 to 90 degrees*		*1.131*
67.6%	*−90 to 90 degrees*		*0.2432*
78.5%	*−90 to 90 degrees*		*−0.0287*
100.0%	*−90 to 90 degrees*		*−0.2977*
Tangential Tilt			
45.5%	*−10 to 10 inches*		*0.0679*
67.6%	*−10 to 10 inches*		*0.0116*
78.5%	*−10 to 10 inches*		*0.0341*
100.0%	*−10 to 10 inches*		*−0.0023*
Axial Tilt			
45.5%	*−10 to 10 inches*		*0.1885*
67.6%	*−10 to 10 inches*		*0.0334*
78.5%	*−10 to 10 inches*		*0.0834*
100.0%	*−10 to 10 inches*		*−0.0036*
Design Constraints	*Limits*	*Initial*	*Final*
Resonances			
1st mode 2E	*0.10 margin*	*−0.0704*	*−0.1146*
2nd mode 4E	*0.05 margin*	*−0.2353*	*−0.2925*
2nd mode 5E	*0.025 margin*	*−0.4033*	*−0.4490*
3rd mode 5E	*0.025 margin*	*−0.1640*	*−0.2680*
Steady Stress (Tsai−Wu)			
Sheath	*1.0*	*0.1325*	*0.3512*
Shell	*1.0*	*0.1862*	*0.5003*
Foam	*1.0*	*0.0048*	*0.0281*
Spar	*1.0*	*0.0086*	*0.0127*
One−P Forced Response			
Life Fraction	*1.0*	*1.5*	*0.7486*
Flutter			
Flutter Mach Number	*0.8*	*0.1063*	*0.1019*
Stall Flutter	*1.0*	*0.3216*	*0.5536*
Driving Power	*2592.*	*2414.*	*2459.*
Objective Function		*0.0479*	*0.0438*

The optimization results of the 18E design are quite impressive. After a total of 147 function calls, which included 10 complete design iterations, the STAT program produced a feasible design with an improved DOC. The blade's stress problems were solved in five complete design moves but then, the power equality constraint became violated. The power constraint and all other constraints were satisfied after the sixth design move was completed. The initial design curves are compared with the optimized curves in Figures 13 through 15, for the blade twist, tangential stacking, and axial stacking, respectively.

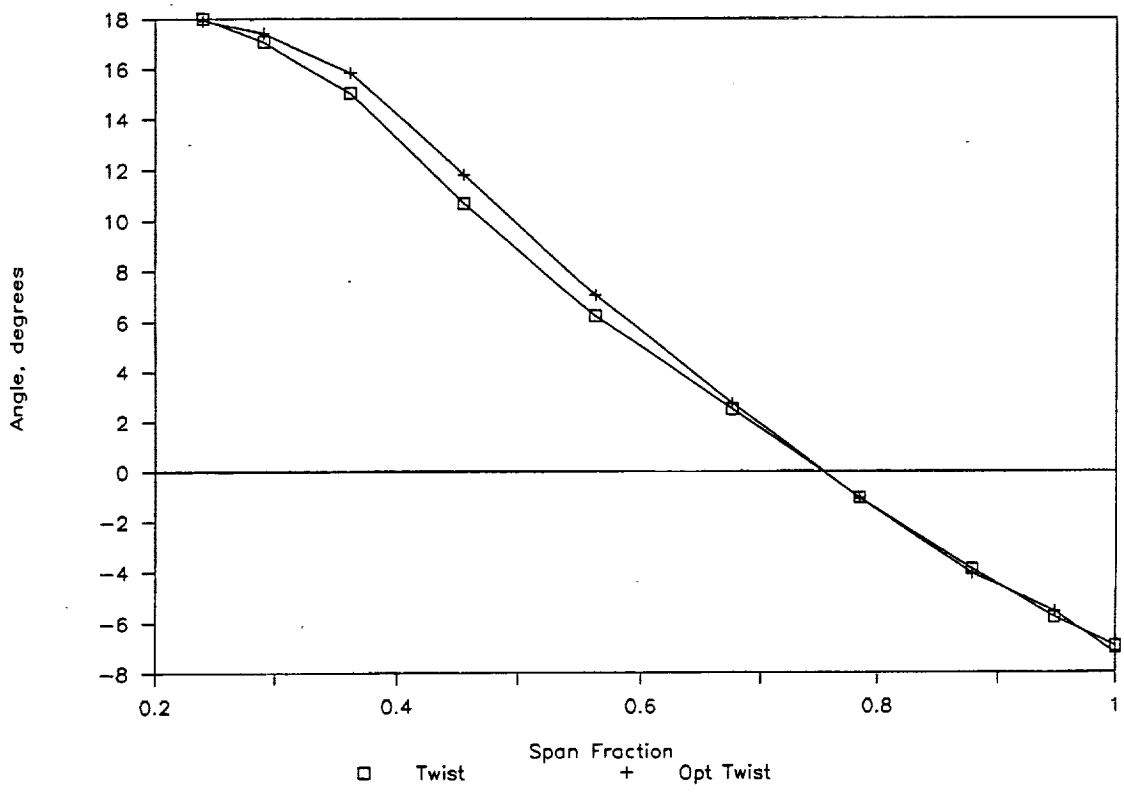

Figure 13. Optimized 18E Propfan Twist

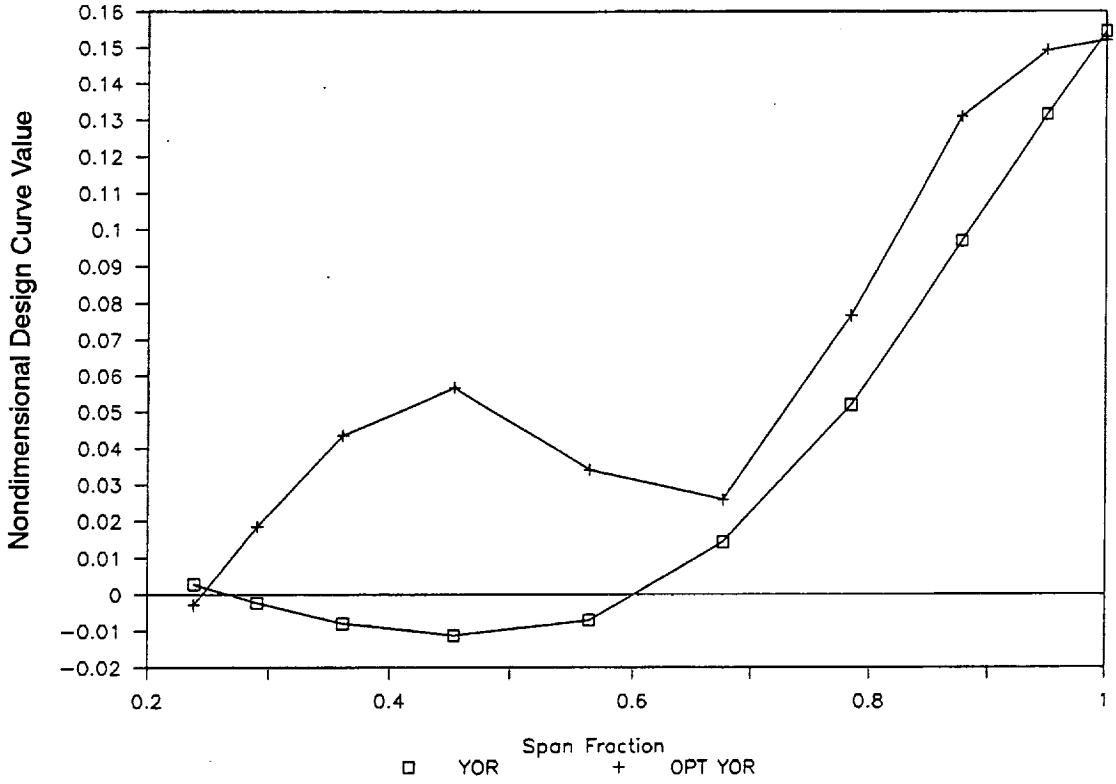

Figure 14. Optimized 18E Propfan Tangential Stacking

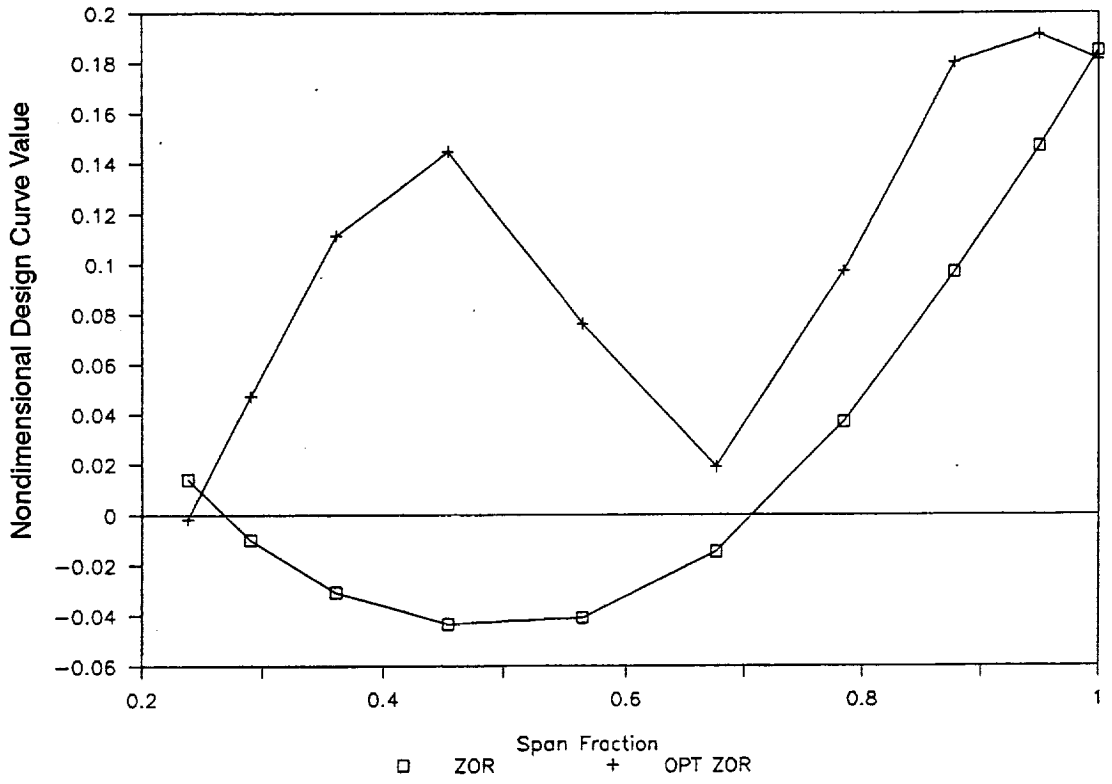

Figure 15. Optimized 18E Propfan Axial Stacking

4.1.2 The SR7 LAP Design

The SR7 design has the identical internal composite construction of the 18E (Figure 4), as well as the same design constraints (Table 5). The blade design differences arise with the external geometry definition. The SR7 and 18E external geometry curves are provided for comparison in Figures 16 to 23.

The SR7 design was optimized using 38 variables which included most all of the parameters necessary to describe the blade. A list of the 38 variables used in the large variable test case is given in Table 7.

Unlike the 18E design, the SR7 LAP blade initially satisfied all of the design constraints. For the large, 38 variable test case, the STAT optimizer was allowed to converge to an optimum design using the ADS algorithm 'Modified Method of Feasible Directions.' The final result was a LAP blade with a DOC improvement of 5.0 percent. However, this particular STAT test case unveiled one of several shortcomings to the new ADS autoscaling procedure. In scaled space, the once-per-revolution forced response life prediction constraint is only slightly violated, such that the optimizer classifies it as an active, not a violated constraint, and thus considers the design as acceptable. However, when the design space is unscaled, the measure of the constraint violation has changed in such a manner as to make it unacceptable.

Because of the violated one-p stress constraint, a second step STAT optimization analysis was performed without the use of ADS autoscaling and using just 12 variables to restack the optimum blade from the prior optimization results to solve the stress problem. STAT was able to quickly find a feasible design, which is summarized in Table 8.

Finally, the results of the STAT SR7 optimization test case were analyzed using refined analyses for the aerodynamic, acoustic, flutter and finite element analyses so as to validate the optimum design. From Table 9, it is obvious that the approximate acoustic analysis is not properly predicting near-field noise trends for changes in blade design. Nevertheless, all of the constraints have remained satisfied and the final refined DOC shows a 3.0 percent improvement over the SR7 design.

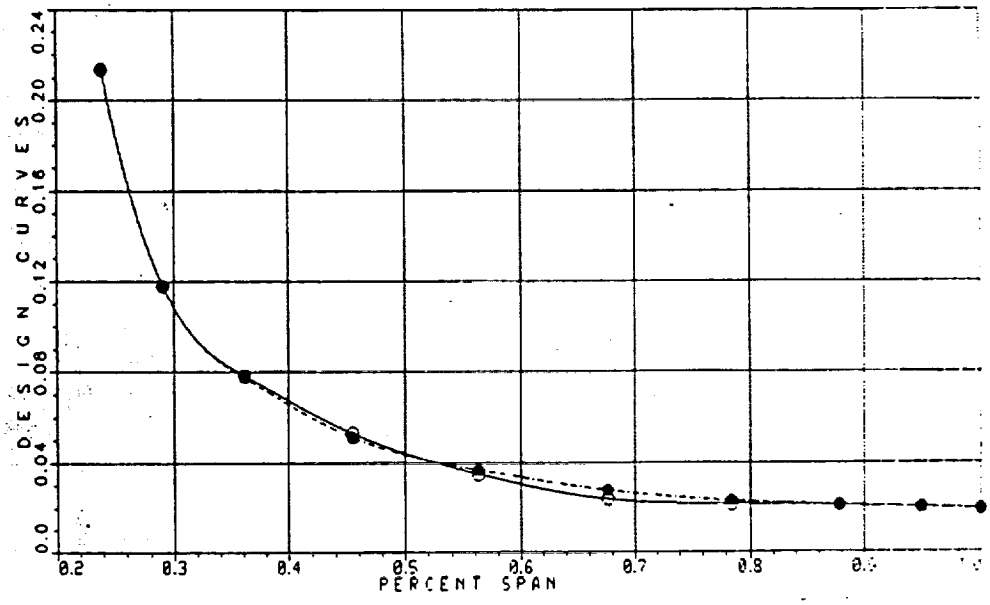

Figure 16. Comparison Overlays of the 18E and SR7 Designs: Thickness/Chord

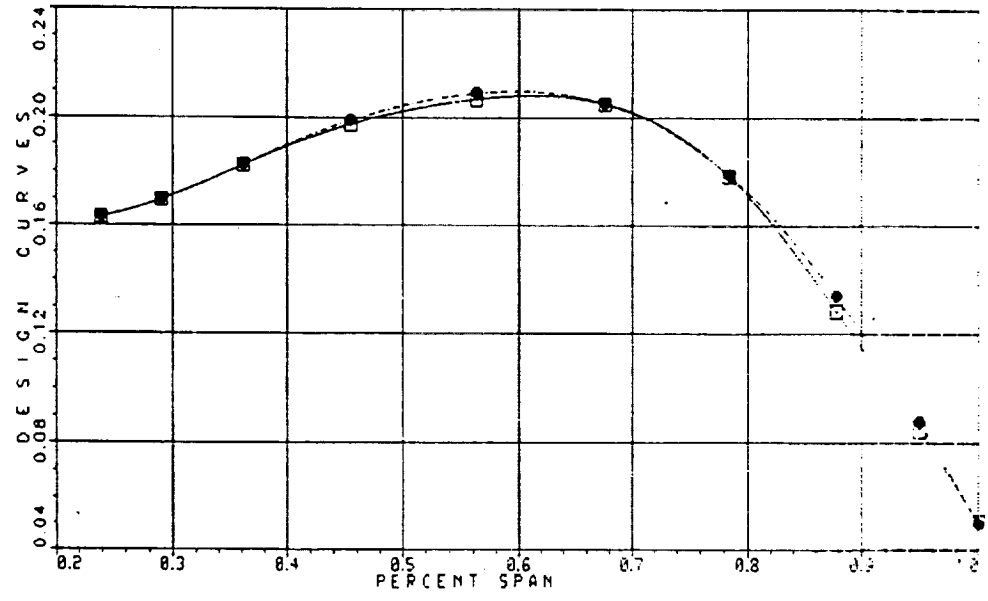

Figure 17. Comparison Overlays of the 18E and SR7 Designs: Chord/Diameter

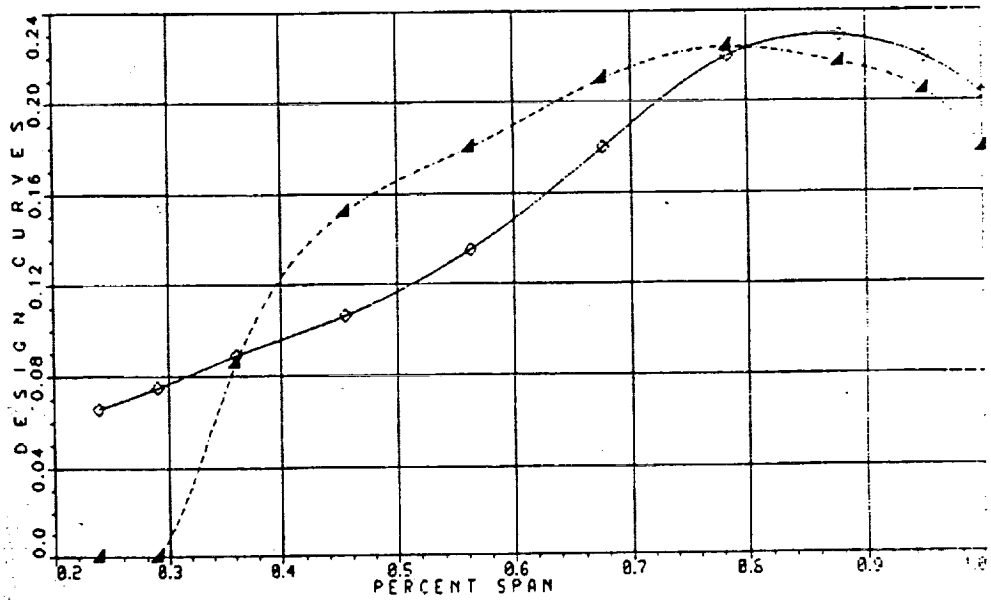

Figure 18. Comparison Overlays of the 18E and SR7 Designs: Camber/Lift Coefficient

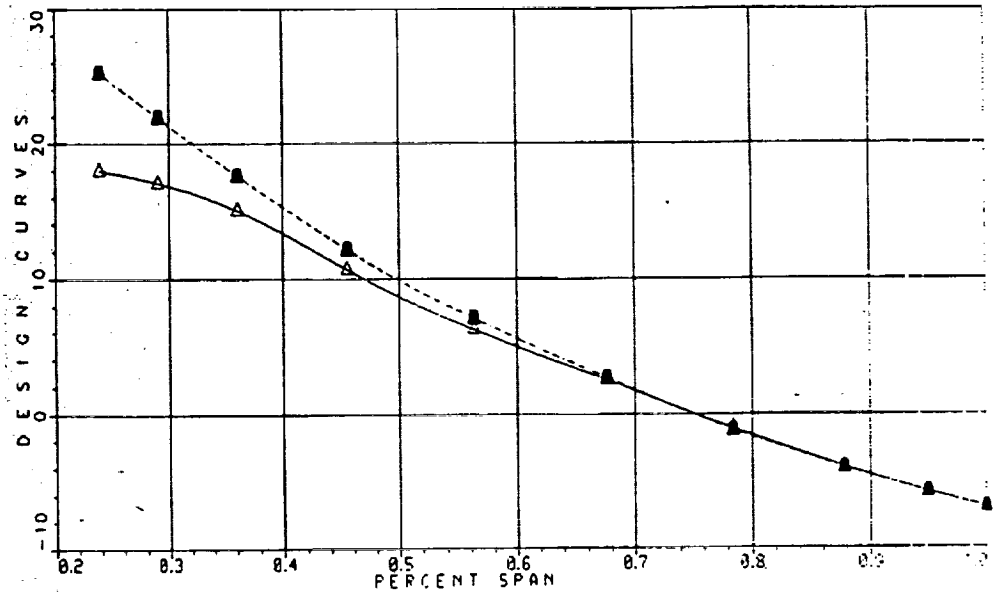

Figure 19. Comparison Overlays of the 18E and SR7 Designs: Blade Twist

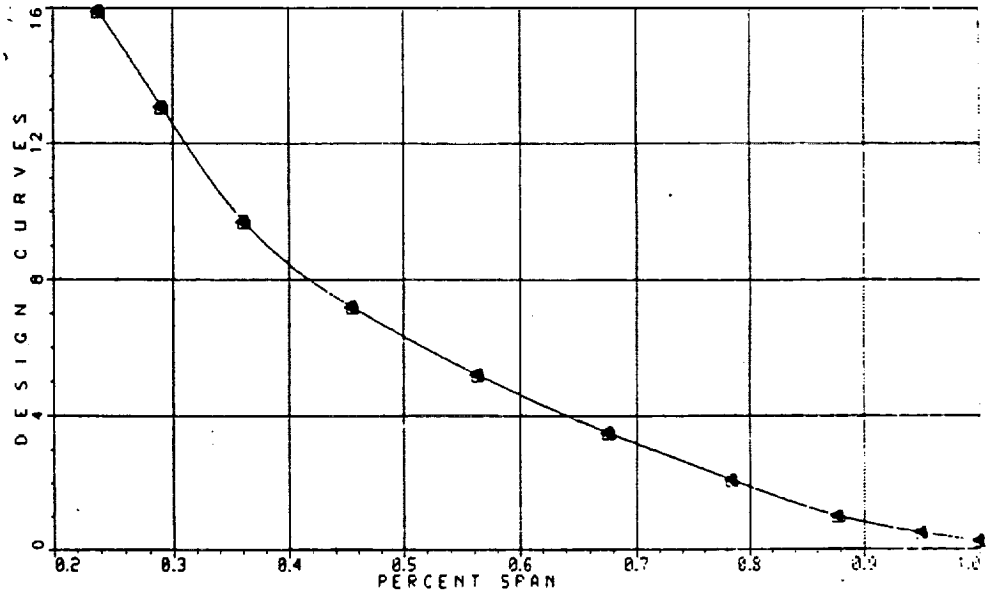

Figure 20. Comparison Overlays of the 18E and SR7 Designs: Conical Section Angle

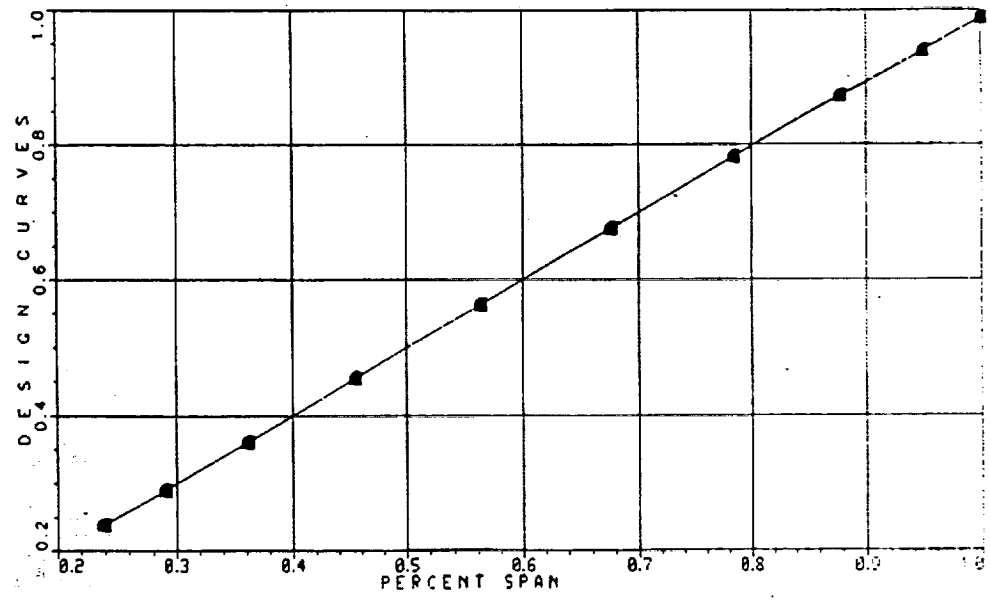

Figure 21. Comparison Overlays of the 18E and SR7 Designs: Radial Stacking

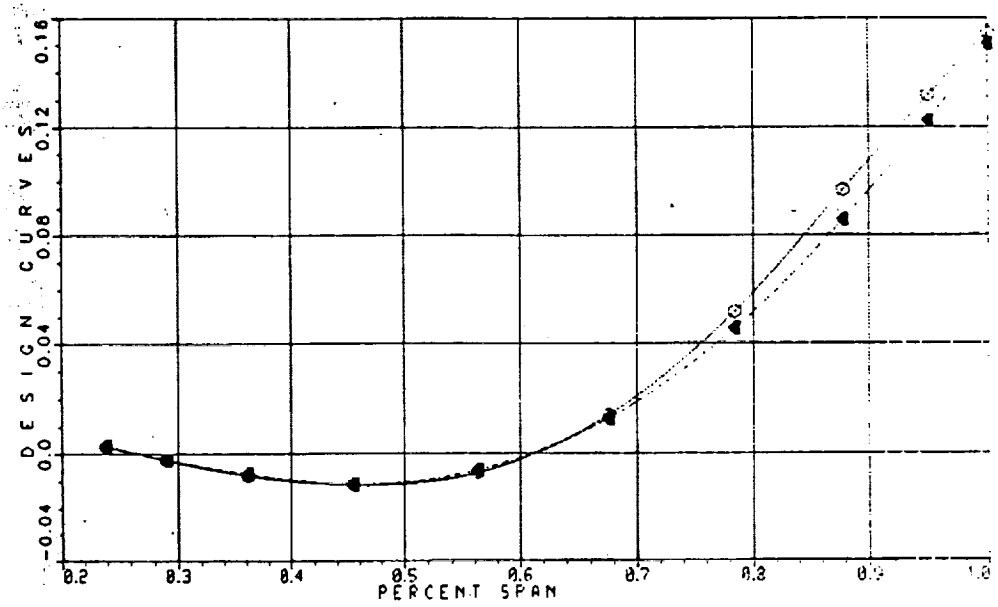

Figure 22. Comparison Overlays of the 18E and SR7 Designs: Tangential Stacking

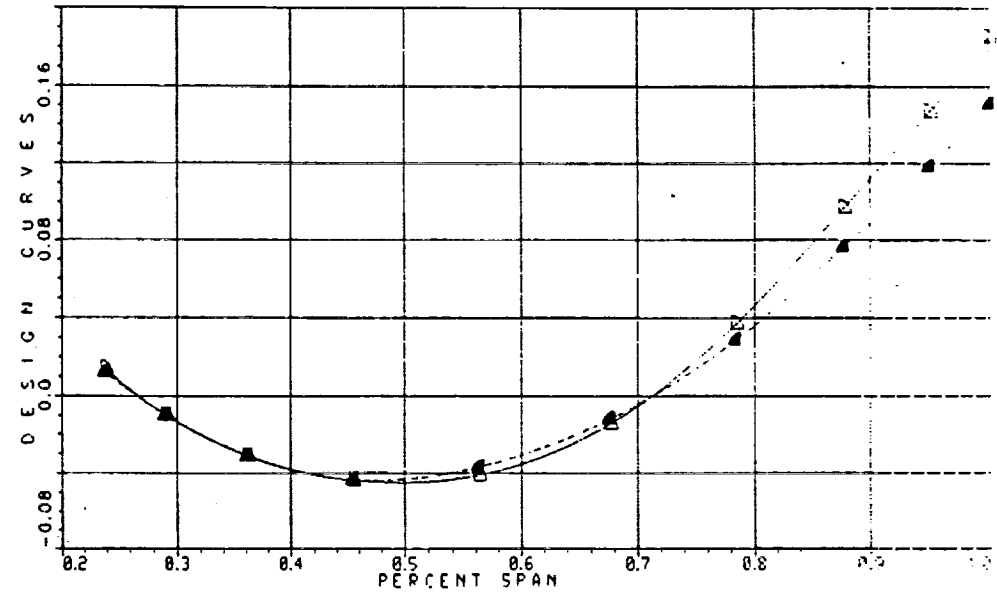

Figure 23. Comparison Overlays of the 18E and SR7 Designs: Axial Stacking

Table 7 The SR7 STAT Optimization Results

Design Variables	Delta Limits	Delta
Exterior Geometry		
Thickness/Chord:		
25% Span	*−0.10 to 0.20*	*0.04677*
43.75% Span	*−0.04 to 0.20*	*−0.00183*
62.5% Span	*−0.02 to 0.20*	*−0.00088*
81.25% Span	*−0.015 to 0.20*	*0.00072*
100.% Span	*−0.005 to 0.20*	*−0.00500*
Chord:		
25% Span	*−16.2 to 2700 inches*	*0.93668*
62.5% Span	*−16.2 to 2700 inches*	*0.03616*
100.% Span	*−4.32 to 2700 inches*	*0.57302*
Lift Coefficient:		
45.47% Span	*−0.15 to 1.0*	*−0.04704*
78.45% Span	*−0.15 to 1.0*	*0.08776*
100.% Span	*−0.15 to 1.0*	*0.28535*
Twist:		
45.47% Span	*−90. to 90. degrees*	*−0.01644*
67.62% Span	*−90. to 90. degrees*	*−0.29220*
78.45% Span	*−90. to 90. degrees*	*0.14895*
100.% Span	*−90. to 90. degrees*	*−0.62752*
Tangential Tilt:		
45.47% Span	*−1.E+5 to 1.E+5 inches*	*0.01603*
67.62% Span	*−1.E+5 to 1.E+5 inches*	*0.06273*
87.80% Span	*−1.E+5 to 1.E+5 inches*	*−0.03222*
100.% Span	*−1.E+5 to 1.E+5 inches*	*0.93204*
Axial Tilt:		
45.47% Span	*−1.E+5 to 1.E+5 inches*	*−0.10362*
67.62% Span	*−1.E+5 to 1.E+5 inches*	*0.21488*
87.80% Span	*−1.E+5 to 1.E+5 inches*	*−0.46021*
100.% Span	*−1.E+5 to 1.E+5 inches*	*0.37737*

* *Active Constraint*
** *Violated Constraint*

Table 7 The SR7 STAT Optimization Results (continued)

Design Variables	*Delta Limits*		*Delta*
Interior Geometry			
Aluminum Spar:			
Spar Meanline:			
25.% Span	*−40. to 40. % chord*		*0.22064*
62.5% Span	*−40. to 40. % chord*		*0.62621*
100.% Span	*−40. to 40. % chord*		*0.63647*
Spar Width:			
25.% Span	*−25. to 25. % chord*		*0.83816*
62.5% Span	*−25. to 25. % chord*		*1.16400*
100.% Span	*−25. to 25. % chord*		*0.04701*
Fiberglass Shell:			
Shell Thickness:			
25.% Span	*−0.03 to 1.0 inch*		*0.00378*
62.5% Span	*−0.03 to 1.0 inch*		*0.00225*
100.% Span	*−0.03 to 1.0 inch*		*−0.01143*
Nickel Sheath:			
Sheath Width:			
50.% Span	*−4.5 to 50. % chord*		*0.00000*
75.% Span	*−12.5 to 50. % chord*		*−1.89890*
100.% Span	*−22.5 to 50. % chord*		*11.20300*
Sheath Thickness:			
50.% Span	*−0.019 to 1.0 inch*		*−0.00175*
75.% Span	*−0.019 to 1.0 inch*		*0.00058*
100.% Span	*−0.019 to 1.0 inch*		*0.00749*
Sheath Cutoff:	*−50. to 50. % span*		*−0.45328*
Design Constraints	*Limits*	*Initial*	*Final*
Resonances:			
1st Mode 2E	*0.10 margin*	*−0.16745*	*−0.19021*
2nd Mode 4E	*0.05 margin*	*−0.30118*	*−0.30302*
2nd Mode 5E	*0.025 margin*	*−0.44095*	*−0.44241*
3rd Mode 5E	*0.025 margin*	*−0.17329*	*−0.13726*

* *Active Constraint*
** *Violated Constraint*

Table 7 The SR7 STAT Optimization Results (continued)

Design Constraints	*Limits*	*Initial*	*Final*
Steady Stress (Tsai–Wu):			
Sheath	*1.0*	*0.04634*	*0.11491*
Shell	*1.0*	*0.05095*	*0.05106*
Foam	*1.0*	*0.00730*	*0.00282*
Spar	*1.0*	*0.00252*	*0.01029*
1–P Force Response Life Fraction	*1.0*	*0.45857*	*1.13282***
Flutter:			
Flutter Mach Number	*1.0*	*1.0332*	*1.0545*
Stall Flutter	*1.0*	*1.7509*	*1.7316*
Driving Power	*2592.*	*2592.*	*2582.2**

Objective Function	*Initial*	*Final*
Direct Operating Cost:		
Efficiency	*0.00004*	*–2.96046*
Noise	*–0.09135*	*–2.02210*
Weight	*–0.03293*	*–0.03627*
Acquisition	*–0.01490*	*–0.01348*
Maintenance	*–0.00546*	*–0.00494*
Total =	*–0.14460*	*–5.03716*
Efficiency (%)	*80.528*	*84.529*
Noise (db)	*143.43*	*139.73*
Weight (lb)	*42.170*	*43.144*

* *Active Constraint*
** *Violated Constraint*

Table 8 The SR7 STAT Optimization to Resolve the Violated Constraint

Design Variables	Initial Delta		Final Delta
Exterior Geometry:			
Twist:	*... degrees*		
45.47% Span	*−0.01644*		*−0.01645*
67.62% Span	*−0.29220*		*−0.29220*
78.45% Span	*0.14895*		*0.14898*
100.% Span	*−0.62752*		*−0.62752*
Tangential Tilt:	*... inches*		
45.47% Span	*0.01603*		*−0.11452*
67.62% Span	*0.06273*		*−0.01893*
87.80% Span	*−0.03222*		*0.34029*
100.% Span	*0.93204*		*0.98172*
Axial Tilt:	*... inches*		
45.47% Span	*−0.10362*		*−0.19449*
67.62% Span	*0.21488*		*0.21457*
87.80% Span	*−0.46021*		*−0.66312*
100.% Span	*0.37737*		*0.56592*
Design Constraints	**Limits**	**Initial**	**Final**
Resonances:			
1st Mode 2E	*0.10 margin*	*−0.19021*	*−0.19091*
2nd Mode 4E	*0.05 margin*	*−0.30302*	*−0.30279*
2nd Mode 5E	*0.025 margin*	*−0.44241*	*−0.44223*
3rd Mode 5E	*0.025 margin*	*−0.13726*	*−0.13636*
Steady Stress (Tsai−Wu):			
Sheath	*1.0*	*0.11491*	*0.08918*
Shell	*1.0*	*0.05106*	*0.04861*
Foam	*1.0*	*0.00282*	*0.00295*
Spar	*1.0*	*0.01029*	*0.00950*
1−P Force Response Life Fraction	*1.0*	*1.13282***	*0.87552*
Flutter:			
Flutter Mach Number	*0.8*	*1.0545*	*1.0882*
Stall Flutter	*1.0*	*1.7316*	*1.7284*
Driving Power	*2592.*	*2582.2**	*2566.3**

* *Active Constraint*
** *Violated Constraint*

Table 8 The SR7 STAT Optimization to Resolve the Violated Constraint (continued)

Objective Function	*Initial*	*Final*
Direct Operating Cost:		
Efficiency	*−2.96046*	*−2.91146*
Noise	*−2.02210*	*−2.53920*
Weight	*−0.03627*	*−0.02423*
Acquisition	*−0.01348*	*−0.01114*
Maintenance	*−0.00494*	*−0.00408*
Total =	*−5.03716*	*−5.49406*
Efficiency (%)	*84.529*	*84.468*
Noise (db)	*139.73*	*138.37*
Weight (lb)	*43.144*	*43.189*

* *Active Constraint*
** *Violated Constraint*

Table 9 *Refined Versus Approximate Analysis for the Initial and Optimum SR7 Designs*

	Hamilton Standard Refined*	STAT Approximate	STAT Refined
Efficiency (%):			
Initial	79.4	80.5	80.1
Optimum		84.5	84.6
Near Field Noise (db):			
Initial	143.	143.4	145.4
Optimum		138.4	146.0
Blade Weight (lb):			
Initial	41.65	42.18	40.45
Optimum		43.19	41.31
Flutter (Mach):			
Initial	0.95	1.033	0.867
Optimum		1.088	0.911
Stall Flutter:			
Initial	**	1.751	1.760
Optimum		1.728	1.694
Driving Power (hp):			
Initial	2592.	2592.	2526.
Optimum		2567.	2506.
Maximum Stress (kpsi):			
Initial	**	11.0	10.6
Optimum		12.0	12.1
Blade Resonances (Hz):			
Initial			
1st Mode	43.2	46.6	46.8
2nd Mode	80.1	78.3	78.0
3rd Mode	101.0	115.7	114.1
Optimum			
1st Mode		45.3	45.6
2nd Mode		78.1	77.5
3rd Mode		120.9	120.4
Blade DOC (%):			
Optimum		−5.6	−3.0

* *Sullivan, W. E., J. E. Turnberg and J. A. Violette, "Large−Scale Advanced Prop−Fan SR−7 Blade," NASA Contract NAS3−23051.*

** *Not available.*

4.1.3 The Aeroelastic Scale Model – The SR7a

The SR7a blade is an aeroelastic scale model representation of the SR7 LAP blade design. The composite aeroelastic scale model (2/9 size) has a total of 12 separate layers. The blade shell is a uniform outer coat of 0.002–inch fiberglass and 3 layers of graphite intertwined among 4 layers of fiberglass cloth. The innermost fiberglass layer is glued to a titanium spar, and the remaining gaps are filled with foam. The spar ends at 80.6 percent span, above which the blade is filled with fiberglass (Figure 24).

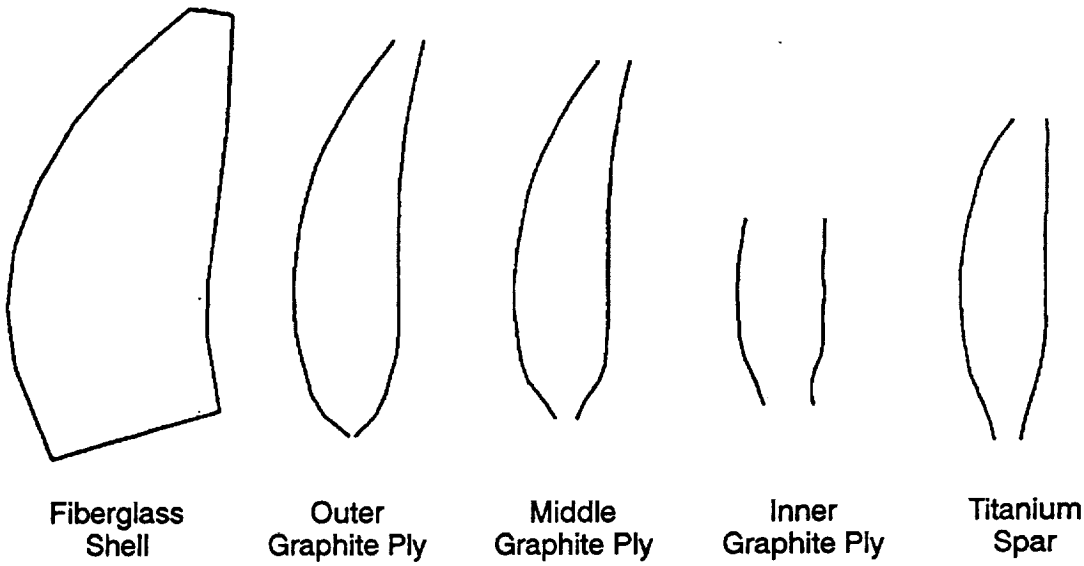

Figure 24. Composite Construction of the SR7a

The exterior geometry of the blade is fixed to that of the SR7 design; therefore, design variables are limited to alterations to the internal construction and the retention stiffness. The design constraints are all weighted into the objective function since, the final optimum will be a model with the identical static and dynamic characteristics of the SR7 design which satisfies all design constraints.

STAT, using the current SR7a geometry as an initial guess to the optimizer, improved the model dramatically in just five complete design moves which involved a total of 213 function calls. The optimizer had not yet converged to an optimum design (i.e., it was allowed to make only five complete design moves) which implies that even greater improvements to the model could have been achieved. The results of this test case show that the objective function definition, as described earlier here within, was adequately structured to properly account for aeroelastic differences between the full scaled blade and its model. The results of the SR7a STAT test case, including a comparison between the SR7 and SR7a aeroelastic properties, are summarized in Table 10 and Figure 25.

Table 10 The SR7a STAT Optimization Results

Design Variables	*Delta Limits*	*Delta*
Attachment		
Diameter	*−1.0 to 2.0 inches*	*−0.05575*
Length	*−1.0 to 2.0 inches*	*−0.06378*
Outer Graphite Ply		
Lower Cutoff	*−100. to 100. % span*	*0.28229*
Upper Cutoff	*−100. to 100. % span*	*4.20610*
Ply Orientation	*−90. to 90. degrees*	*1.26720*
Ply Meanline:		
30.% Span	*−25. to 25. % chord*	*0.72419*
60.% Span	*−25. to 25. % chord*	*16.47200*
90.% Span	*−25. to 25. % chord*	*7.09530*
Ply Width:		
30.% Span	*−25. to 25. % chord*	*0.22693*
60.% Span	*−25. to 25. % chord*	*10.22300*
90.% Span	*−25. to 25. % chord*	*4.24170*
Middle Graphite Ply		
Lower Cutoff	*−100. to 100. % span*	*−5.32560*
Upper Cutoff	*−100. to 100. % span*	*5.05070*
Ply Orientation	*−90. to 90. degrees*	*−1.00770*
Ply Meanline:		
35.% Span	*−25. to 25. % chord*	*2.17050*
60.% Span	*−25. to 25. % chord*	*1.04900*
85.% Span	*−25. to 25. % chord*	*1.79730*
Ply Width:		
35.% Span	*−25. to 25. % chord*	*−0.13600*
60.% Span	*−25. to 25. % chord*	*2.46400*
85.% Span	*−25. to 25. % chord*	*2.60010*
Inner Graphite Ply		
Lower Cutoff	*−100. to 100. % span*	*−4.82330*
Upper Cutoff	*−100. to 100. % span*	*−0.71739*
Ply Orientation	*−90. to 90. degrees*	*0.30925*
Ply Meanline:		
35.% Span	*−25. to 25. % chord*	*1.23910*
47.5% Span	*−25. to 25. % chord*	*3.07600*
60.% Span	*−25. to 25. % chord*	*0.39277*

Table 10 The SR7a STAT Optimization Results (continued)

Design Variables	*Delta Limits*		*Delta*
Ply Width:			
35.% Span	*−25. to 25. % chord*		*0.21038*
47.5% Span	*−25. to 25. % chord*		*2.36390*
60.% Span	*−25. to 25. % chord*		*−0.03735*
Titanium Spar			
Upper Cutoff	*−100. to 100. % span*		*1.89600*
Spar Meanline:			
25.% Span	*−25. to 25. % chord*		*−4.02210*
50.% Span	*−25. to 25. % chord*		*24.42800*
75.% Span	*−25. to 25. % chord*		*−5.91010*
Spar Width:			
25.% Span	*−25. to 25. % chord*		*−2.09210*
50.% Span	*−25. to 25. % chord*		*6.26880*
75.% Span	*−25. to 25. % chord*		*1.77210*
Fiberglass Filler Lower Cutoff	*−100. to 100. % span*		*−1.68310*
Objective Function	*Initial*		*Final*
Mass Distribution	*0.44986*		*0.41948*
Resonances	*0.02914*		*0.00620*
Static Deflection	*0.03898*		*0.13837*
Modal Deflection	*1.22790*		*0.62513*
Total Value =	*1.7485*		*1.1892*
SR7, SR7a Comparison	*SR7*	*SR7a Initial*	*SR7a Final*
Efficiency (%)	*81.589*	*82.695*	*81.644*
Noise (db)	*143.44*	*143.24*	*143.47*
Weight (lb)	*42.170*	*0.52737*	*0.45596*
	Times Scale Factor Cubed:	*45.174*	*39.057*
Driving Power (hp)	*2592.0*	*2453.4*	*2593.4*
Flutter Mach Number	*1.0332*	*1.0733*	*1.0051*
Stall Flutter	*1.7509*	*1.5782*	*1.6375*
Resonances:			
1st Mode	*46.623*	*218.59*	*206.12*
	Divided by Scale Factor:	*49.588*	*46.759*
2nd Mode	*78.267*	*399.44*	*372.09*
	Divided by Scale Factor:	*90.614*	*84.409*
3rd Mode	*115.74*	*502.78*	*507.19*
	Divided by Scale Factor:	*114.06*	*115.06*

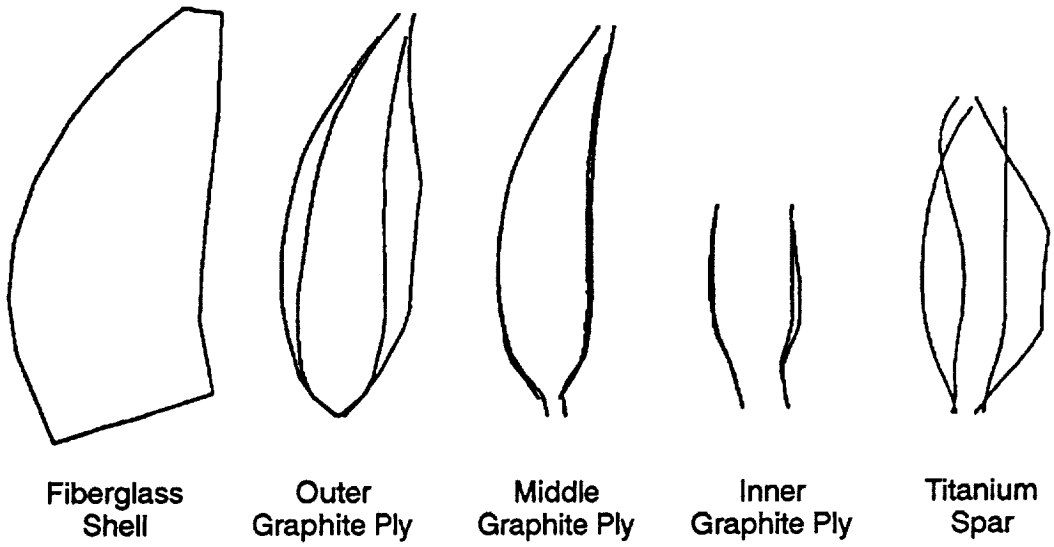

Figure 25. Initial and Optimum Design Composite Construction Overlay Plots of the SR7a

4.2 Counter–Rotation Propfan Applications

To evaluate STAT's performance for the optimization of counter–rotating propfans (CRP), the program was applied to two configurations – a full size CRP, and a scale model CRP.

4.2.1 Full Size Counter–Rotation Propfan

Prior to application of the STAT program, Hamilton Standard had never designed a full size CRP – all CRP experience had been on scale model configurations, in particular the 17 percent size aerodynamic scale model CRPX1. To generate a full size CRP design, the scale model CRPX1 geometry was expanded to full size (12.0 ft tip diameter). A spar–shell construction, similar to the SR–7 SRP, was selected. Thus, it was likely that the newly developed full size CRP would not meet design structural requirements.

The blade is of a composite construction incorporating a nickel sheath layer for protection against foreign object damage, a fiberglass outer shell, an internal aluminum spar, and foam used to fill the gaps between the spar and the shell to prevent localized shell buckling. The overall construction of the blade is shown in Figure 26, which includes the chordal projection of the shell, along with overlays of the sheath and the spar. The shell thickness tapers along the span, as shown in Figure 27. Both front and rear blades are assumed to have similar composite construction.

The external geometry of each rotor is defined by eight spanwise distribution curves that include blade stacking, twist, chord, thickness, and other pertinent parameters. Figure 28 shows the spanwise distributions of the twist (beta) and cone angles for the front blade. Figure 29 shows the thickness (HOB), chord (BOD), and lift coefficient (CLD) distributions for the front airfoil. Figure 30 shows the front blade X stacking, and Figure 31 shows the tangential (YOR) and axial (ZOR) stacking distributions. Figures 32 through 35 show the corresponding geometry definitions for the rear rotor of CRP1.

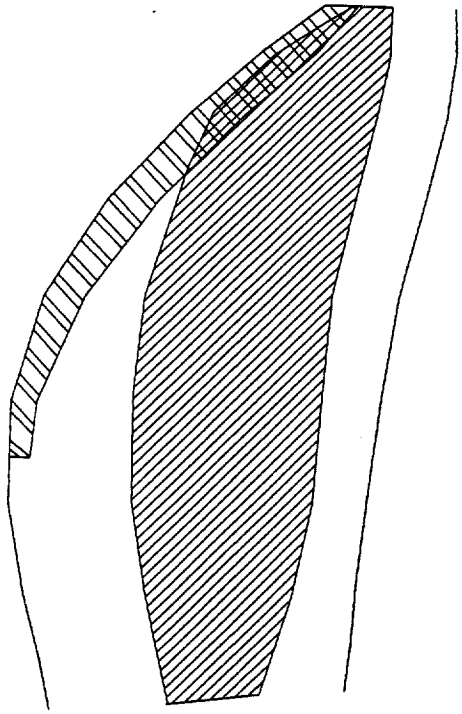

Figure 26. Full Size CRP Composite Construction Planform

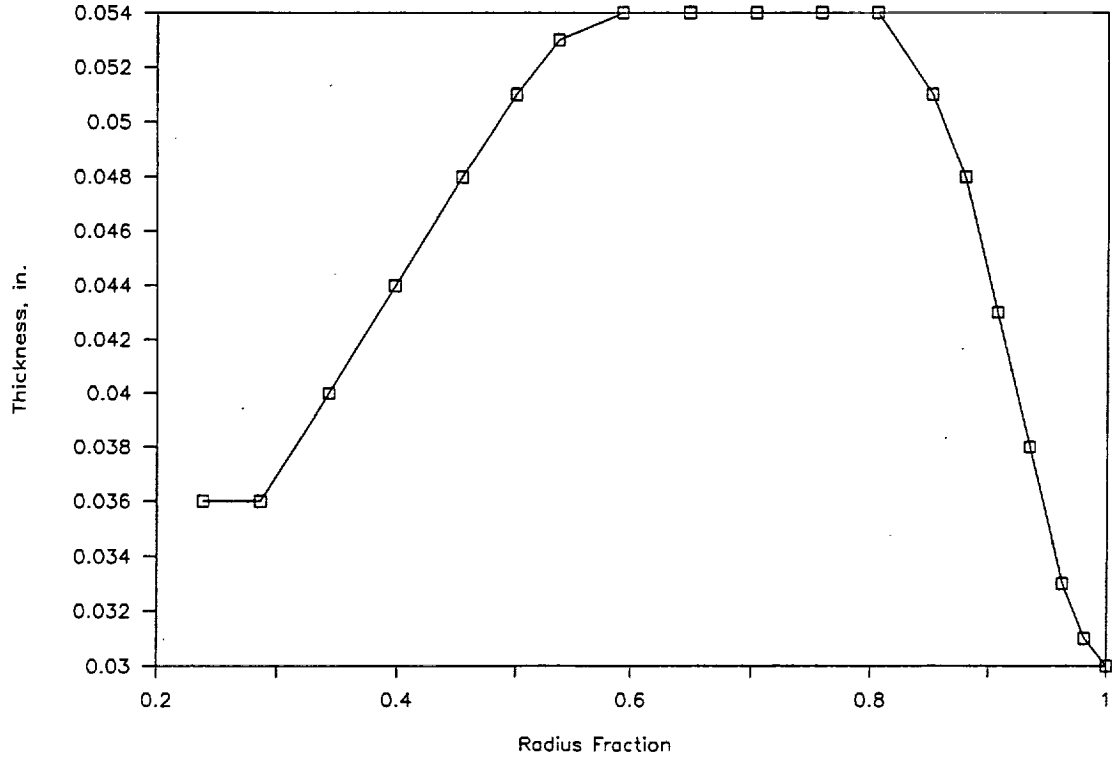

Figure 27. Full Size CRP Shell Thickness Distribution

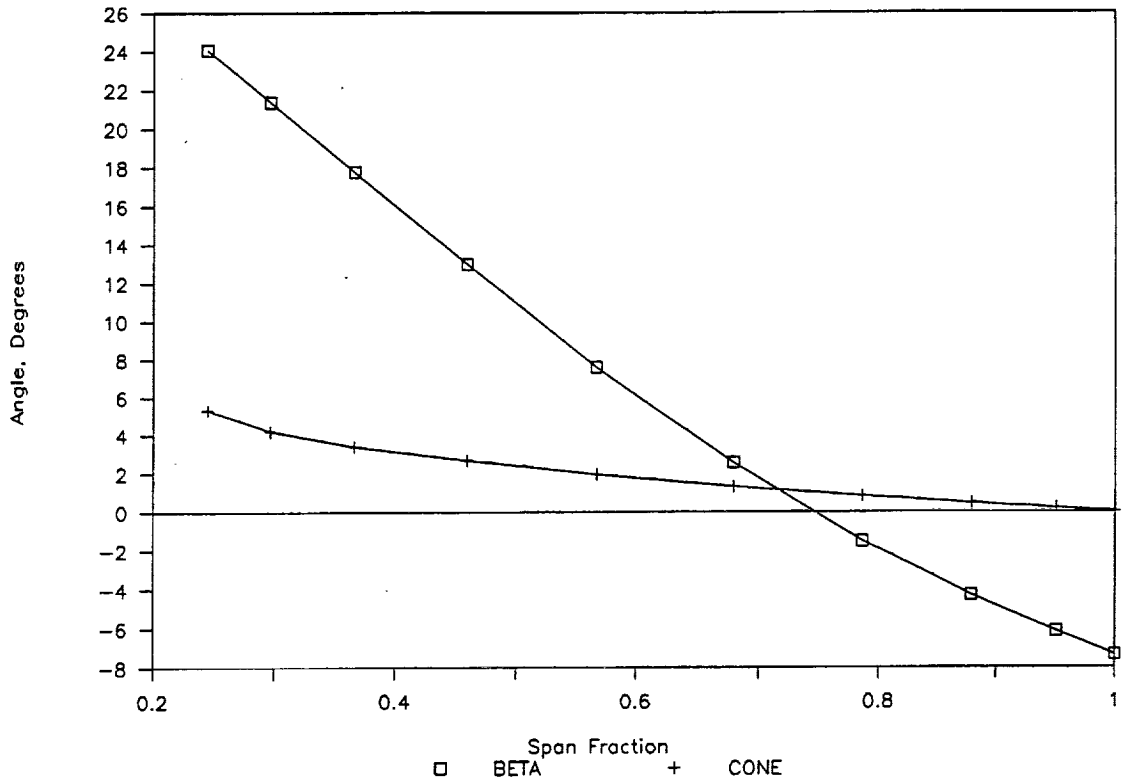

Figure 28. Full Size CRP Front Blade Twist and Cone Angle Distributions

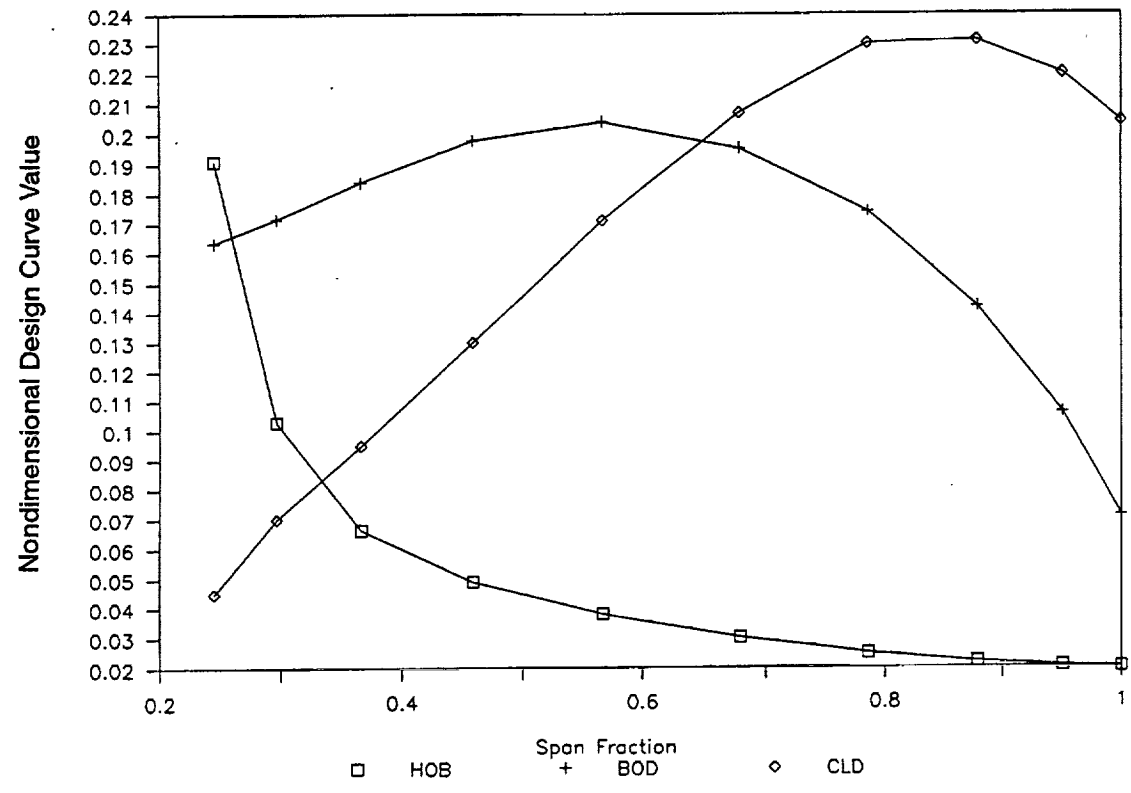

Figure 29. Full Size CRP Front Blade Thickness, Chord, and Lift Coefficient Distributions

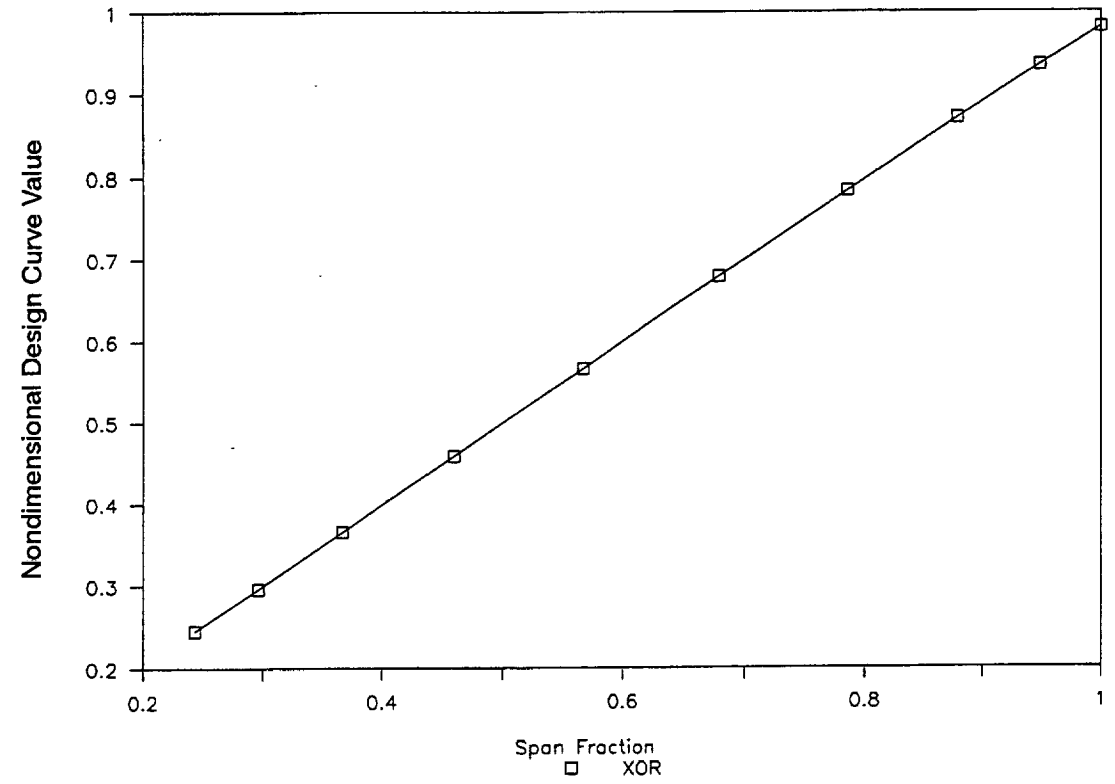

Figure 30. Full Size CRP Front Blade Radial Stacking Distribution

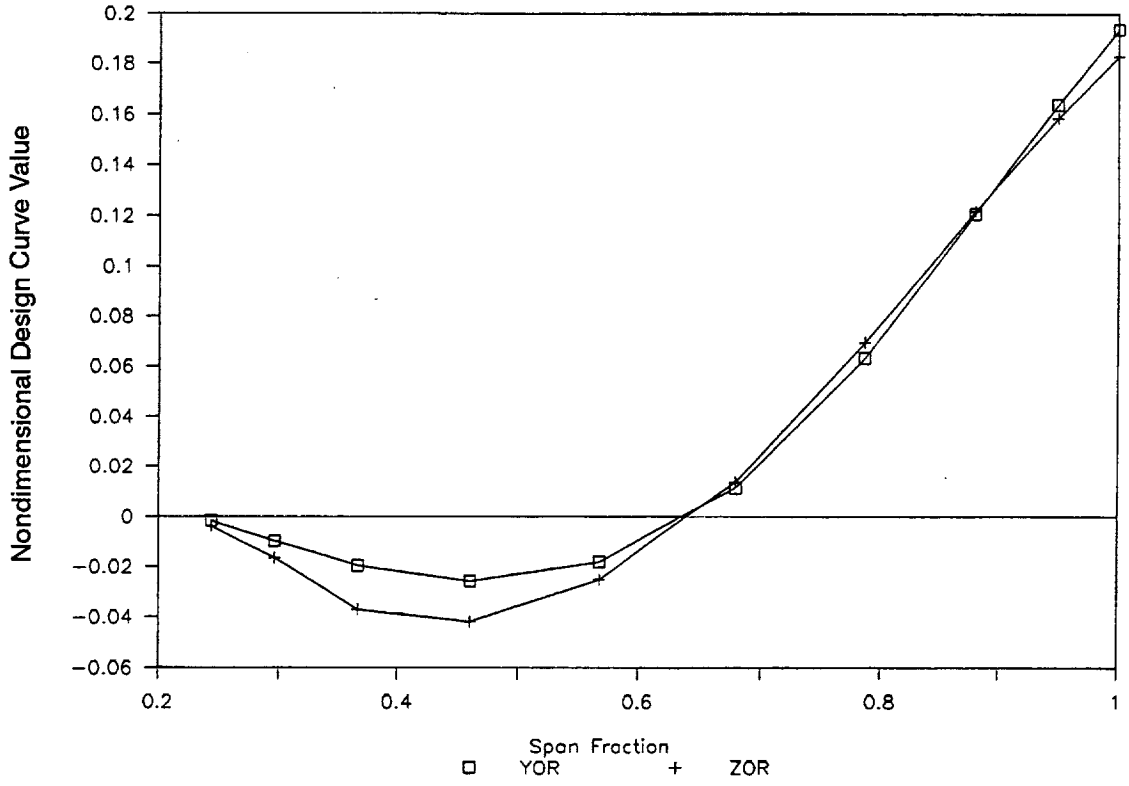

Figure 31. Full Size CRP Front Blade Tangential and Axial Stacking Distributions

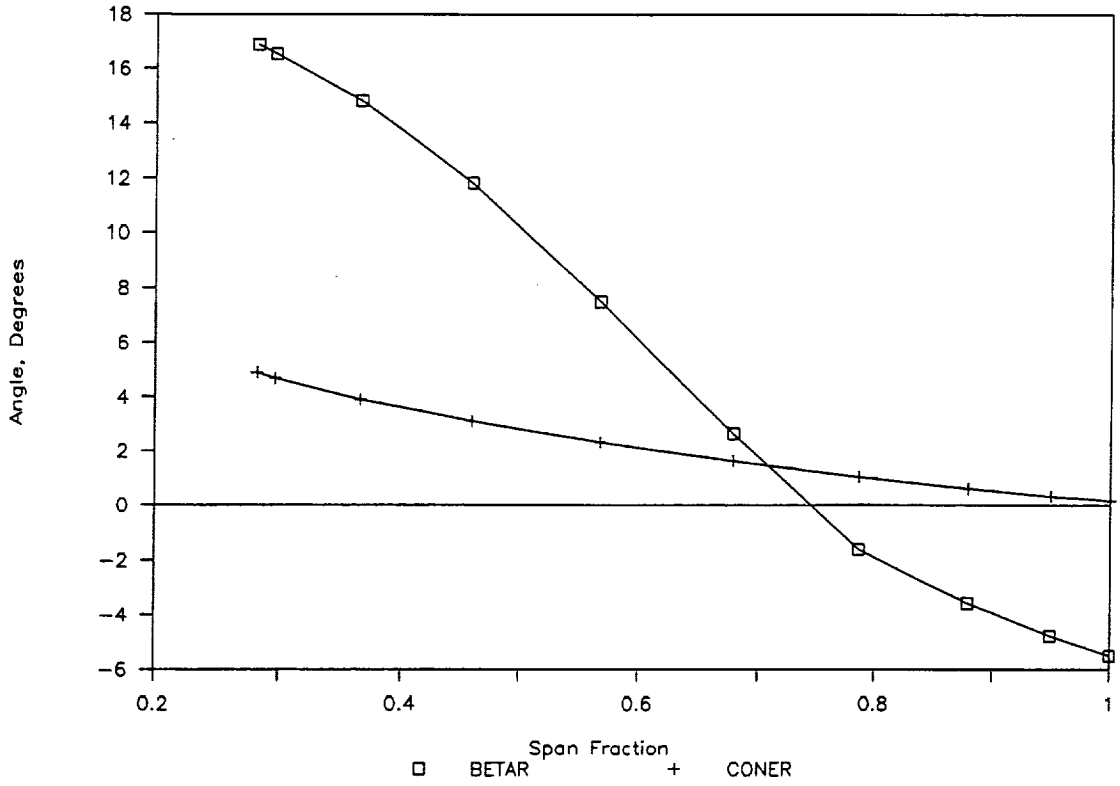

Figure 32. Full Size CRP Rear Blade Twist and Cone Angle Distributions

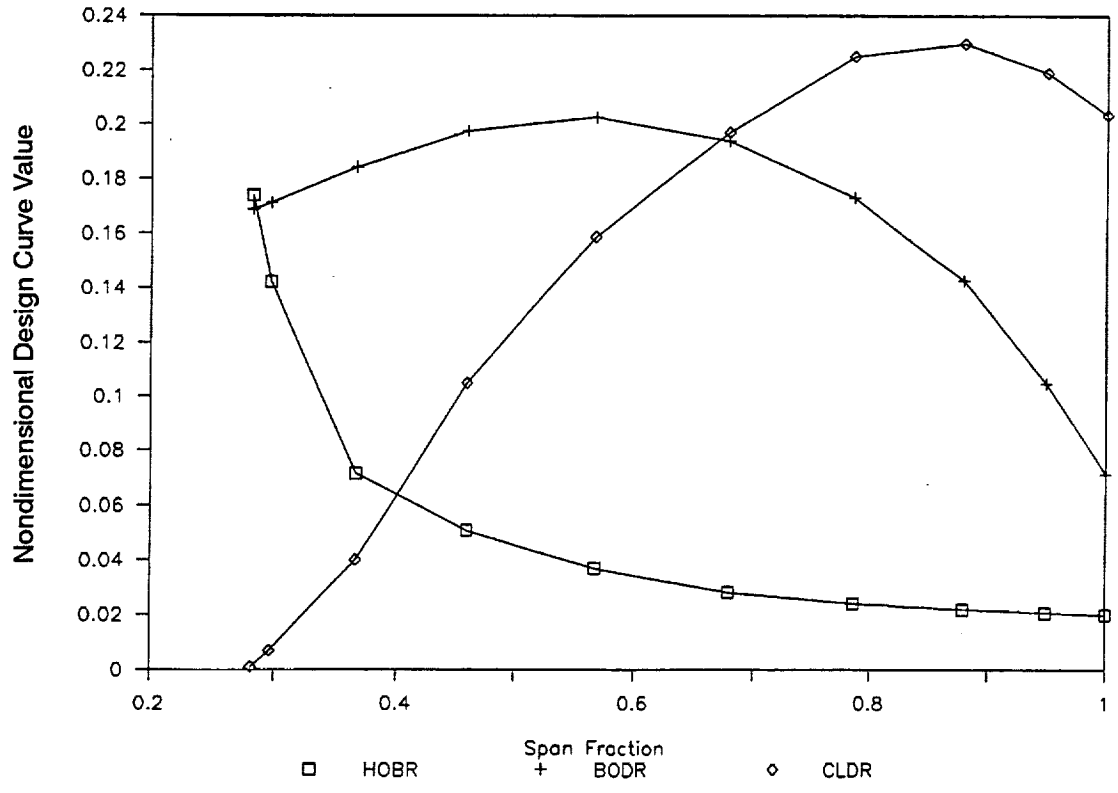

Figure 33. Full Size CRP Rear Blade Thickness, Chord, and Lift Coefficient Distributions

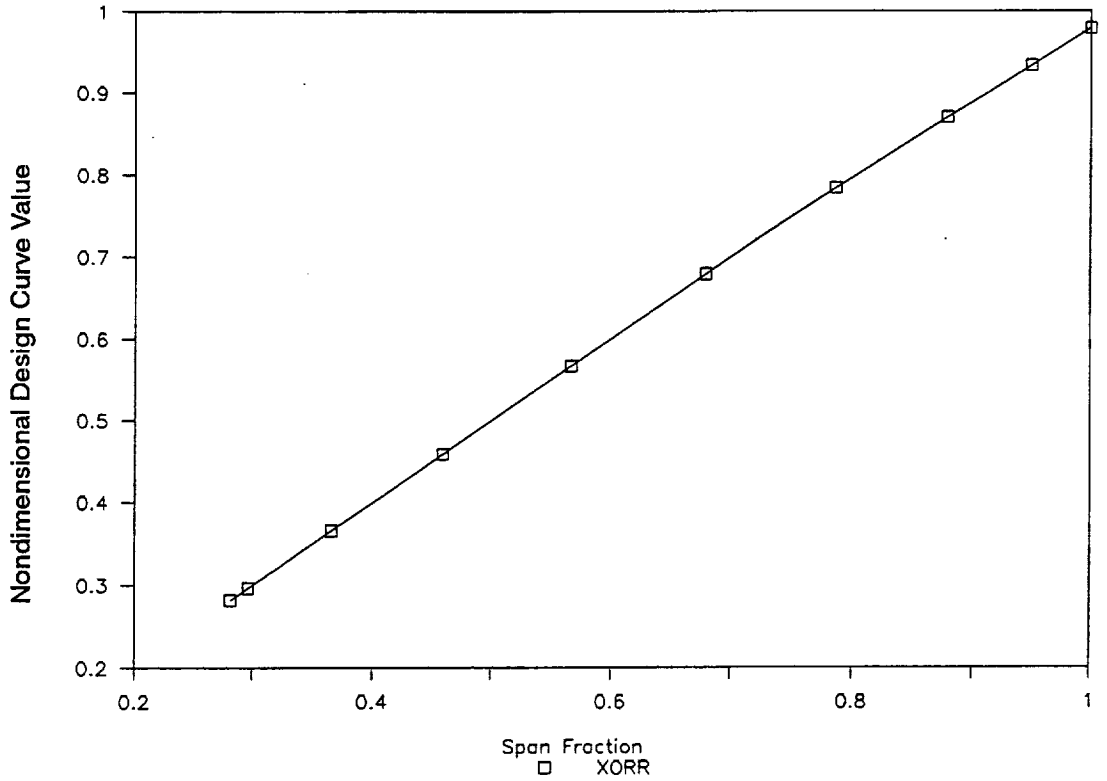

Figure 34. Full Size CRP Rear Blade Radial Stacking Distribution

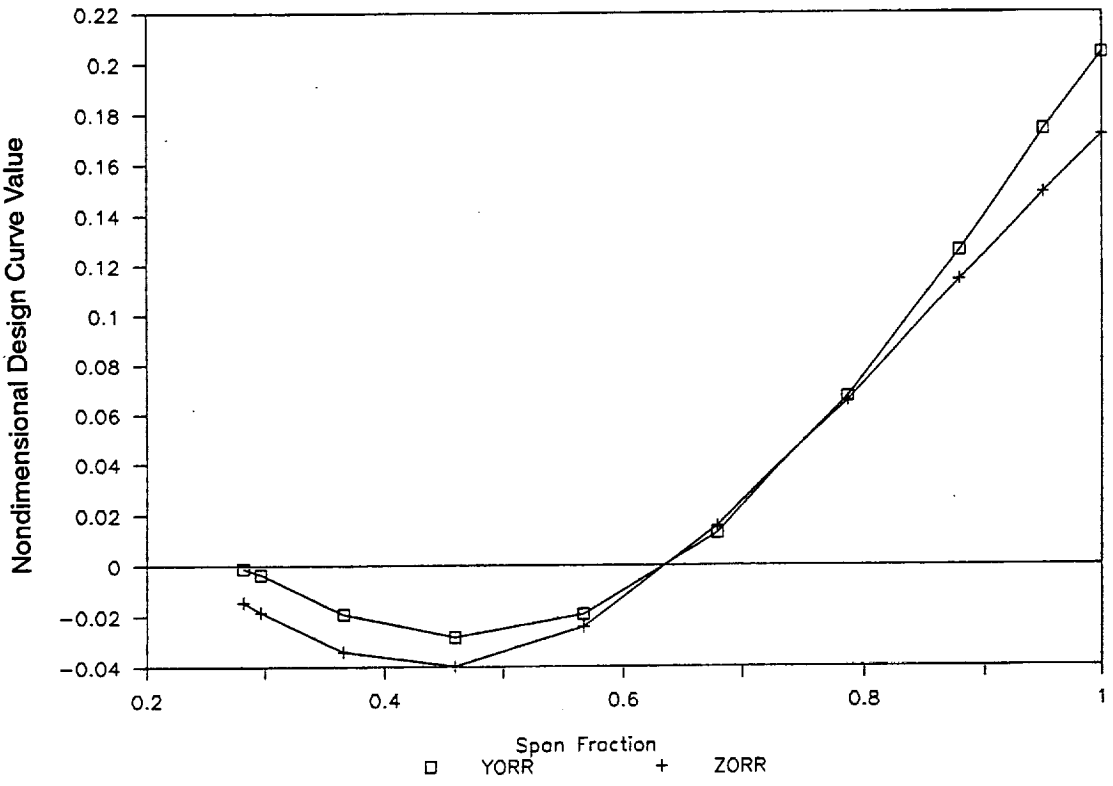

Figure 35. Full Size CRP Rear Blade Tangential and Axial Stacking Distributions

Constraints applied to the CRP1 design optimization apply to both rotor stages, as well as to the rotor system. The constraints include limits on the blade geometry, vibratory resonance margins, static stress, once–per–revolution forced response life, classical flutter Mach number, stall flutter parameter, and rotor power. Thus, all the constraints normally associated with the propfan design process have been applied to this design optimization. The CRP1 design constraints are detailed in Table 11.

Table 11 CRP1 Design Constraints

Blade Geometry

- *Thickness/chord minimums to avoid local airfoil buckling*
- *Realistic upper and lower limits for all design curves*
- *Maintain root stacking position relative to blade attachment*

Blade Flutter

- *Classical flutter Mach number > 1.0*
- *Stall flutter parameter > 1.0*

Power

- *Front rotor power of 5349.6 hp*
- *Rear rotor power of 5349.6 hp*

Blade Resonance Margins

- *1st mode 2P – 10%*
- *2nd mode 5P – 2.5%*
- *3rd mode 5P – 2.5%*

Blade Stresses

- *Tsai–Wu layer steady stress factor < 1.0*
- *Once–per–revolution forced response life fraction < 1.0*

The first step in the blade optimization process is to evaluate the initial design configuration. The base CRP1 did not have the correct power output, and the once–per–revolution stresses were excessive. To correct this design limitation, the optimization process was employed.

The objective function for the optimization was to minimize a combination of efficiency and weight, equal to:

$$DOC = 0.0013 * (\text{System Weight, lb}) - 74 * (\text{System Efficiency}).$$

This trade of weight and efficiency is the same objective used in the SR7 SRP optimizations.

To adjust the propfan power output, the most powerful design variable is twist angle. To control stresses, tangential and axial tilts have powerful effects. Thus, each blade was given a number of these quantities to treat as design variables. Additionally, spar width and chordwise position and shell thickness were allowed to vary. This provides additional stress and frequency tuning capability to the STAT design optimization process. The full set of design variables, along with their respective spanwise positions and variation limits are listed in Table 12.

Table 12 CRP1 Design Variables

Design Variable	*% Span Location*	*Lower and Upper Limit*
Front Twist	*45.47*	*−90. to +90. degrees*
	78.45	*−90. to +90. degrees*
	100.0	*−90. to +90. degrees*
Front Tangential Tilt	*67.62*	*−0.1 to +0.1 inches*
	100.0	*−0.1 to +0.1 inches*
Front Axial Tilt	*67.62*	*−0.1 to +0.1 inches*
	100.0	*−0.1 to +0.1 inches*
Rear Twist	*67.62*	*−90. to +90. degrees*
	100.0	*−90. to +90. degrees*
Rear Tangential Tilt	*67.62*	*−0.1 to +0.1 inches*
	100.0	*−0.1 to +0.1 inches*
Rear Axial Tilt	*67.62*	*−0.1 to +0.1 inches*
	100.0	*−0.1 to +0.1 inches*
Spar Meanline	*23.89*	*−0.4 to +0.4 (chord fraction)*
	64.81	*−0.4 to +0.4 (chord fraction)*
	100.0	*−0.4 to +0.4 (chord fraction)*
Spar Width	*23.89*	*−0.25 to +0.25 (chord)*
	64.81	*−0.25 to +0.25 (chord)*
	100.0	*−0.25 to +0.25 (chord)*
Shell Thickness	*23.89*	*−0.02 to +1.0 inches*
	64.81	*−0.02 to +1.0 inches*
	100.0	*−0.02 to +1.0 inches*

With the above listed 22 design variables, a STAT optimization of the CRP1 blade was executed. STAT terminated, having found its candidate optimum, on analysis #281. This analysis included 39 design candidates. The remainder of the analysis calls were gradient evaluations. The final values for the design variables are listed in Table 13. To even find a feasible design was quite a chore – STAT's first feasible design was on analysis #200.

Table 13 CRP1 Optimization – Design Variable Changes

Design Variable	*Final Value*	*Variable*	*Final Value*
Front Twist:		*Rear Twist:*	
45%	*2.5969*	*68%*	*0.1268*
78%	*−0.0600*	*100%*	*−0.0573*
100%	*0.1347*	*Rear Tangential Tilt:*	
Front Tangential Tilt:		*68%*	*0.00047*
68%	*0.00059*	*100%*	*−0.02491*
100%	*−0.05759*	*Rear Axial Tilt:*	
Front Axial Tilt:		*68%*	*0.00041*
68%	*−0.00005*	*100%*	*−0.00146*
100%	*0.02123*		
Spar Meanline:			
24%	*−0.01435*		
65%	*−0.02183*		
100%	*−0.00568*		
Spar Width:			
24%	*0.01154*		
65%	*0.02312*		
100%	*0.00099*		
Shell Thickness:			
24%	*0.00088*		
65%	*0.00060*		
100%	*0.00058*		

Table 14 compares the performance characteristics of the initial CRP1 design with those of the optimized rotor system.

Table 14 CRP1 Optimization – Constraint Values

Constraint	Limit	Initial Design	Optimal Design
Front Blade			
Resonances:			
1st Mode 2P	*221 (U)*	*32*	*33*
2nd Mode 5P	*600 (U)*	*81*	*85*
3rd Mode 5P	*600 (U)*	*105*	*113*
Steady Stress (Tsai–Wu):			
Sheath	*1.0 (U)*	*0.1743*	*0.2138*
Shell	*1.0 (U)*	*0.3873*	*0.0604*
Spar	*1.0 (U)*	*0.0149*	*0.0161*
Foam	*1.0 (U)*	*0.0085*	*0.0033*
Flutter:			
Flutter Mach Number	*1.0 (L)*	*1.95*	*1.95*
Stall Flutter Parameter	*1.0 (L)*	*1.46*	*1.71*
1–P Forced Response Life Fraction	*1.0 (U)*	*3.155 – V*	*0.995 – A*
Driving Power (hp)	*5350 (E)*	*3113 – V*	*4975 – A*
Weight (lb)		*105*	*111*
Efficiency (%)		*0.813*	*0.735*
Near–Field Noise (db)		*138*	*139*
Rear Blade			
Resonances:			
1st Mode 2P	*221 (U)*	*32*	*34*
2nd Mode 5P	*600 (U)*	*82*	*85*
3rd Mode 5P	*600 (U)*	*99*	*101*
Steady Stress (Tsai–Wu):			
Sheath	*1.0 (U)*	*0.4953*	*0.1280*
Shell	*1.0 (U)*	*0.4026*	*0.1201*
Spar	*1.0 (U)*	*0.0123*	*0.0107*
Foam	*1.0 (U)*	*0.0087*	*0.0064*

Where: *(L) – denotes lower limit*
(U) – denotes upper limit
(L) – denotes equality constraint
V – denotes violated constraint
A – denotes active constraint

Table 14 CRP1 Optimization – Constraint Values (continued)

Constraint	Limit	Initial Design	Optimal Design
Flutter:			
Flutter Mach Number	*1.0 (L)*	*1.95*	*1.80*
Stall Flutter Parameter	*1.0 (L)*	*1.36*	*1.40*
1–P Forced Response Life Fraction	*1.0 (U)*	*3.99 – V*	*0.964 – A*
Driving Power (hp)	*5350 (E)*	*4159 – V*	*5813 – A*
Weight (lb)		*95*	*100*
Efficiency (%)		*0.834*	*0.789*
Near–Field Noise (db)		*138*	*140*
CRP Rotor System:			
Net Efficiency		*0.825*	*0.764*
Objective Function		*0.254*	*0.269*

Where: *(L) – denotes lower limit*
(U) – denotes upper limit
(L) – denotes equality constraint
V – denotes violated constraint
A – denotes active constraint

The updates made to the CRP1 design curves by the STAT program are illustrated in Figures 36 through 43. Figure 36 shows the optimized spar chordal planform (solid line), compared with the original planform (dotted line). Figure 37 shows the changes made by STAT to the front airfoil twist distribution. As shown on Figure 38, the rear blade twist was adjusted only slightly. Figure 39 shows that significant changes were made to the front blade tangential stacking. The rear prop tangential stacking was much less altered, as shown on Figure 40. The airfoil axial stackings were much less altered, as shown on Figure 41 for the front blade, and Figure 42 for the rear. The final curve to be updated by the CRP1 optimization was the shell thickness. Figure 43 shows the slight overall shell thickness increase prescribed by the STAT optimization process.

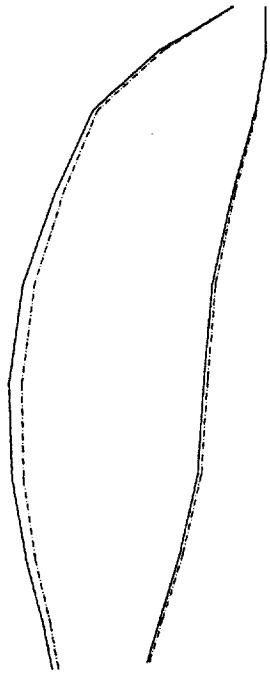

Figure 36. Optimized CRP1 Spar Chordal Planform

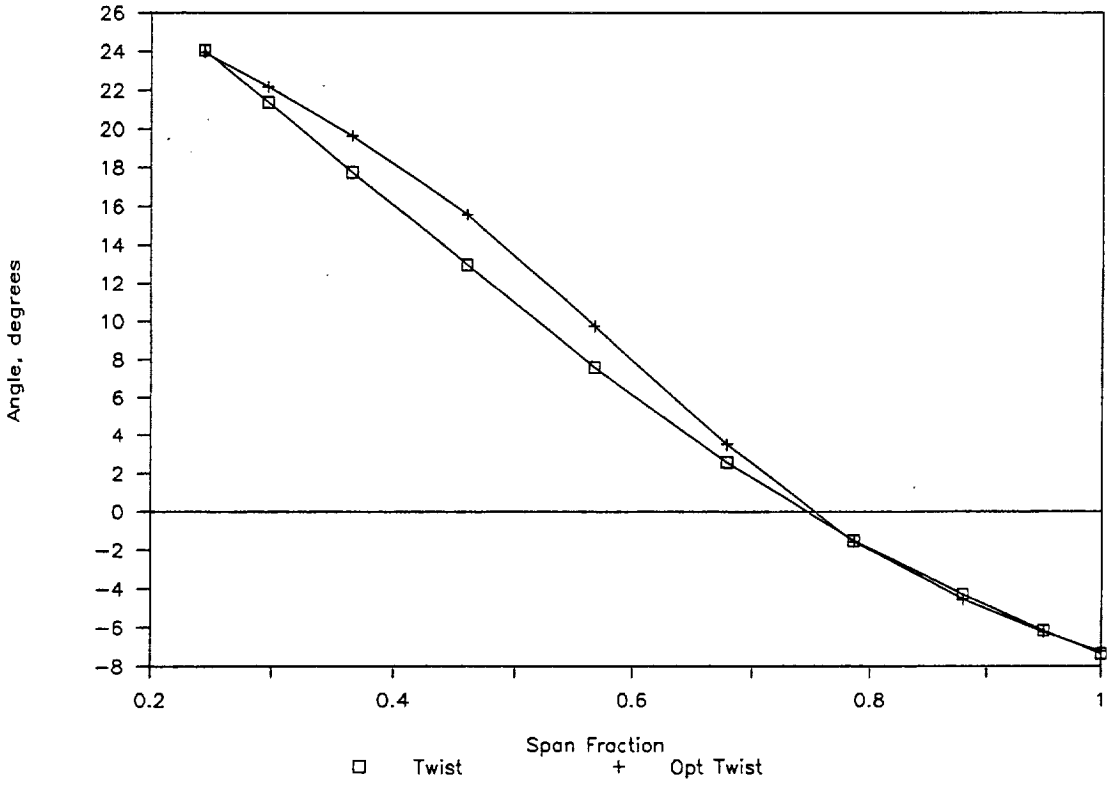

Figure 37. Optimized CRP1 Front Blade Twist Distribution

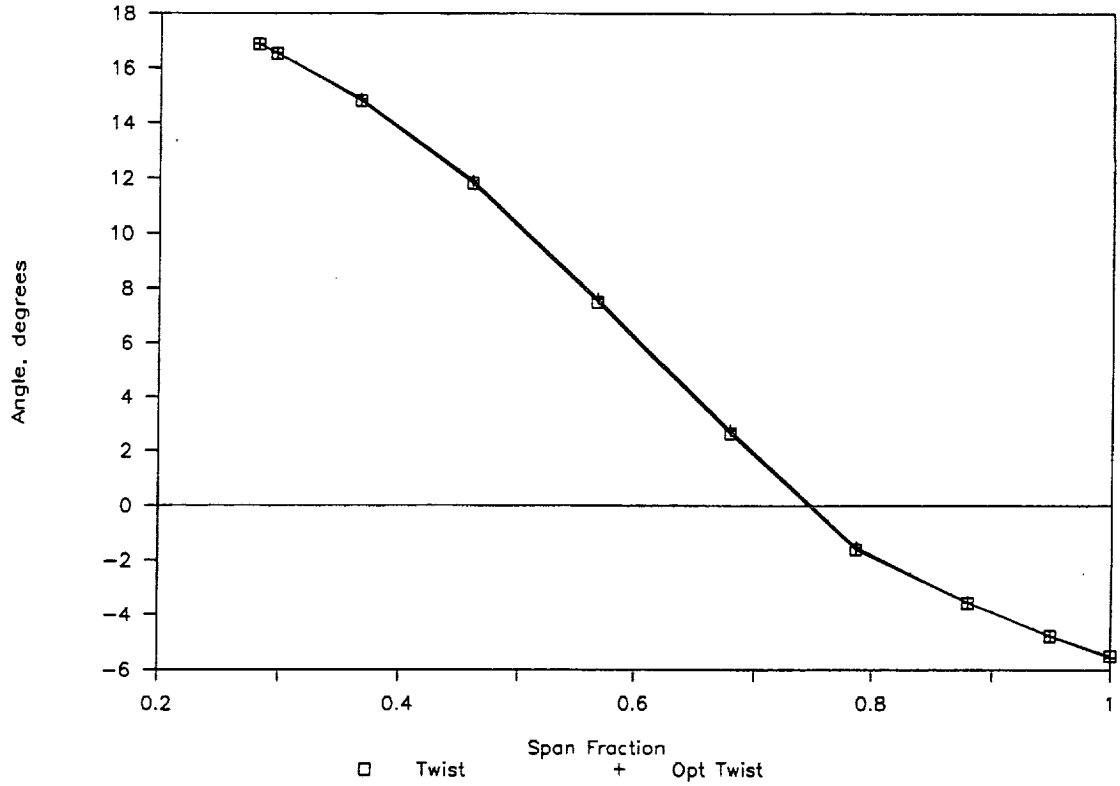

Figure 38. Optimized CRP1 Rear Blade Twist Distribution

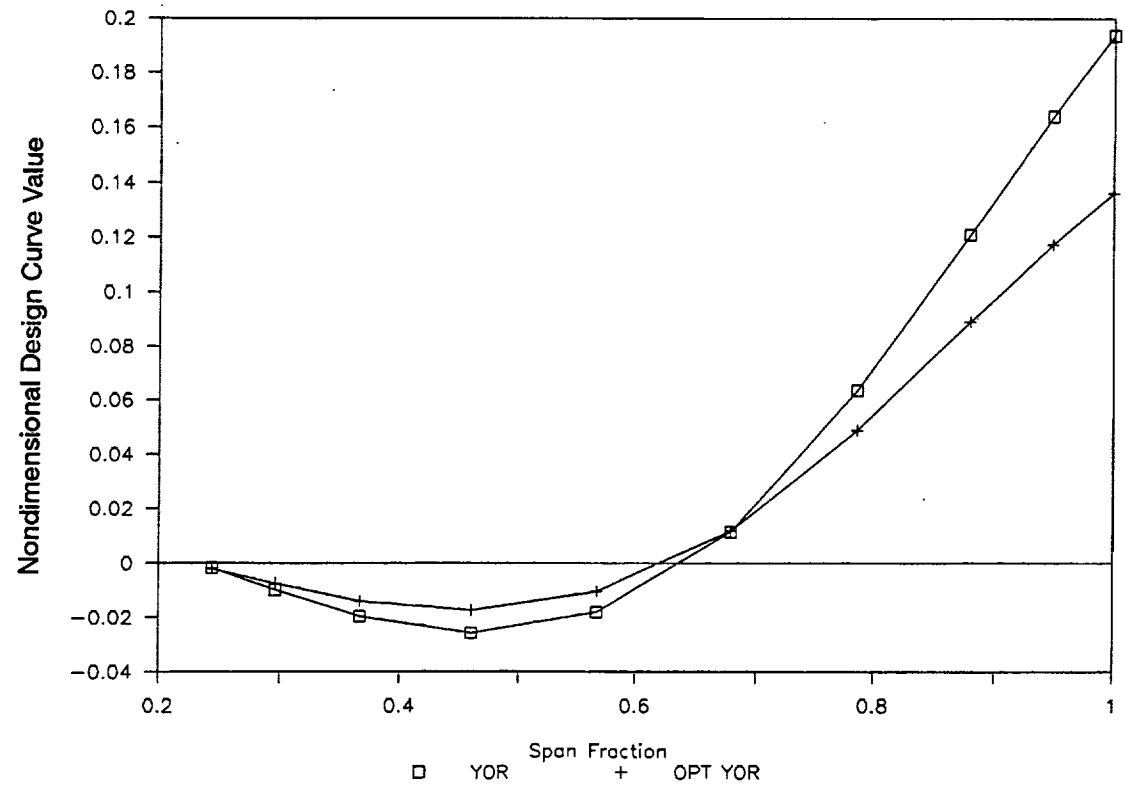

Figure 39. Optimized CRP1 Front Blade Tangential Stacking

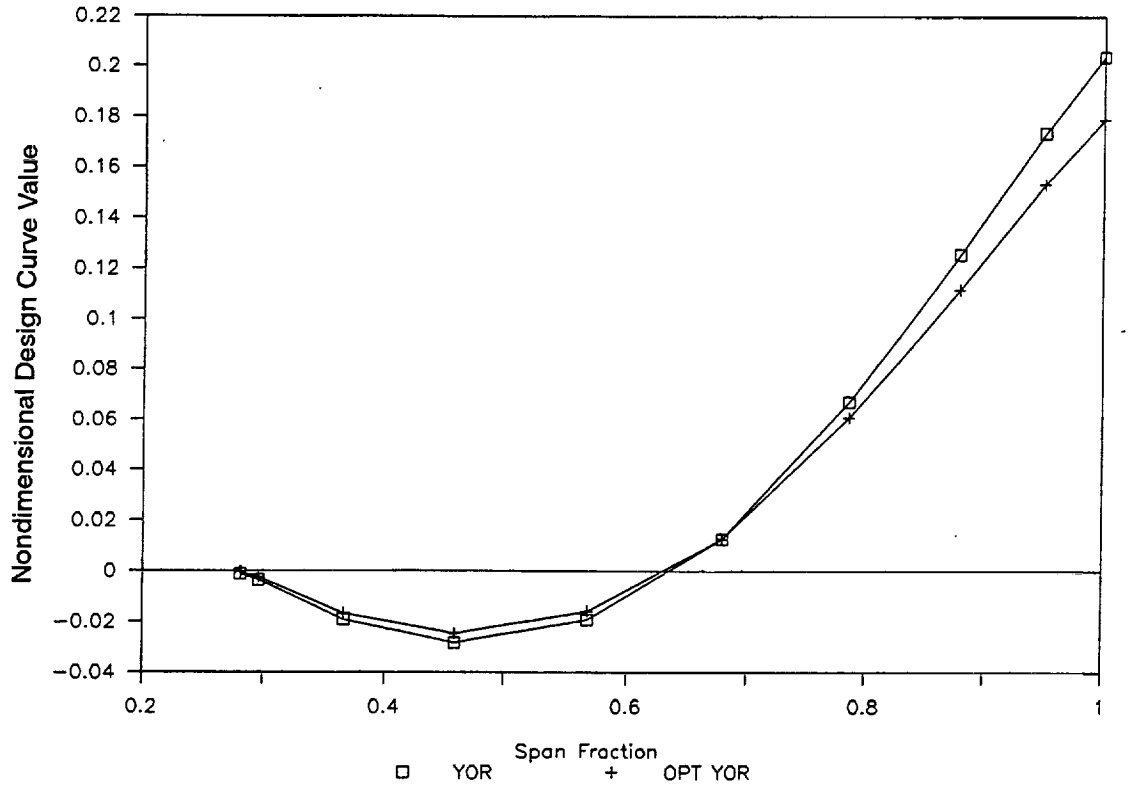

Figure 40. Optimized CRP1 Rear Blade Tangential Stacking

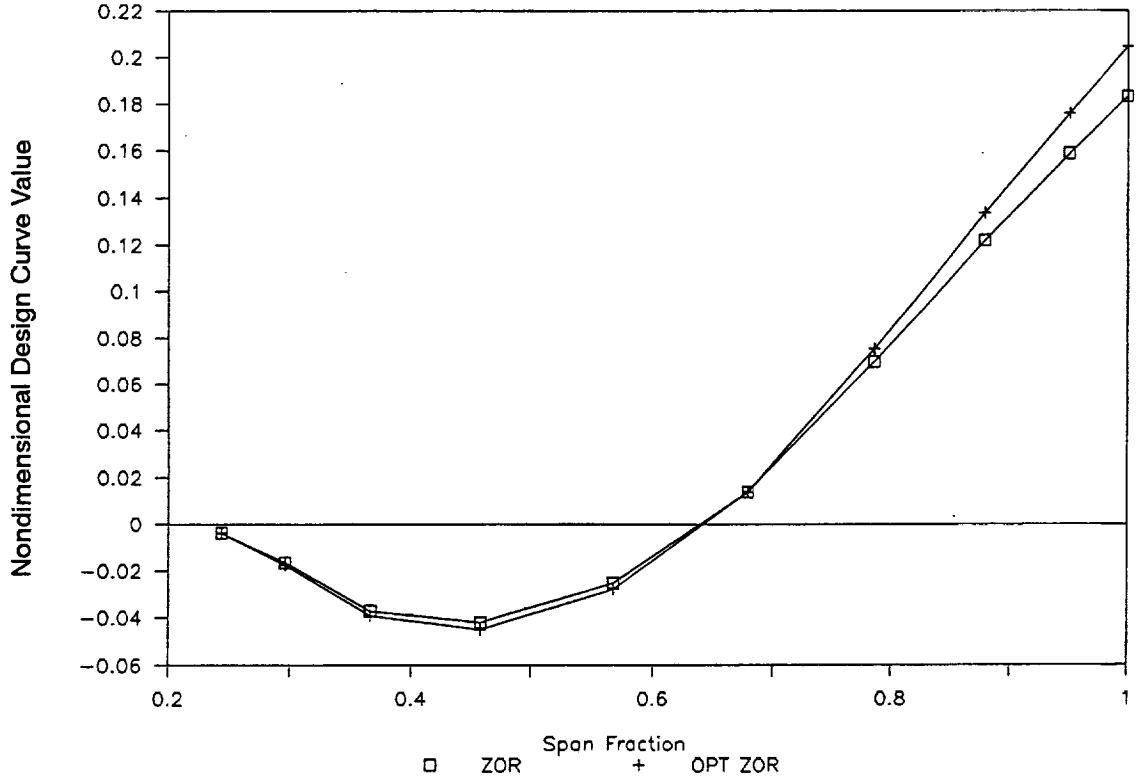

Figure 41. Optimized CRP1 Front Blade Axial Stacking

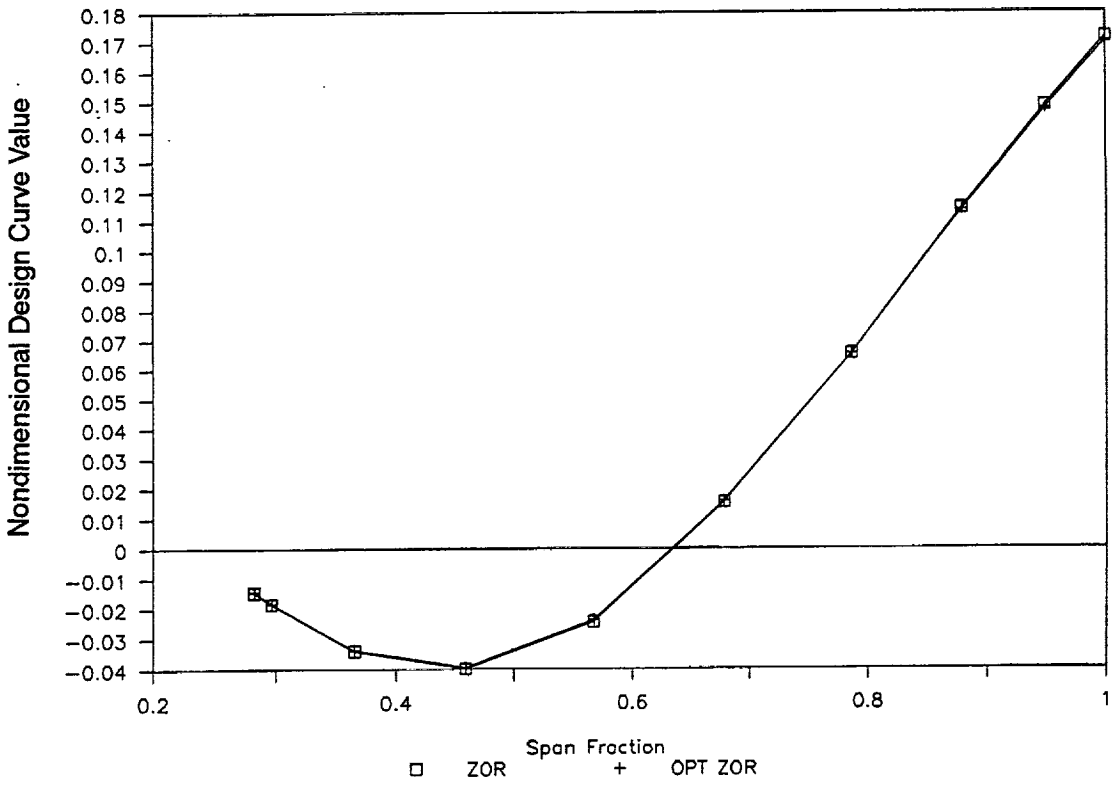

Figure 42. Optimized CRP1 Rear Blade Axial Stacking

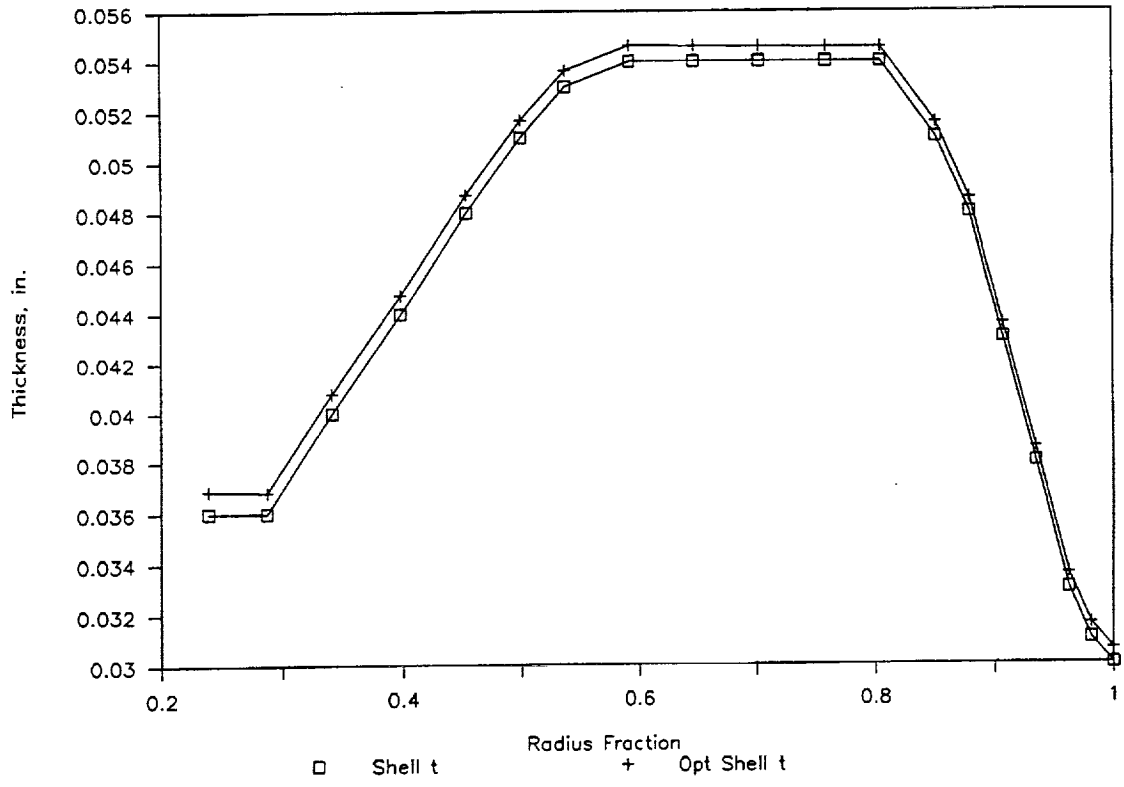

Figure 43. Optimized CRP1 Shell Thickness Distribution

4.2.2 Scale Model Counter Rotation Propfan

The CRP1 optimization of Section 4.2.1 having established a viable counter rotation propfan rotor set, it is now reasonable to ask STAT to develop an appropriate aero–elastic scale model of CRP1 for wind tunnel validation and performance test. The aerodynamic similarity optimization capability of STAT permits just such a process.

Where the full size CRP1 was a composite shell on a metallic spar construction with foam fill, the reduced diameter of the scale size wind tunnel somewhat restricts the available design freedoms of the STAT program, limiting us to laminated composite constructions. The external shape of the scale model is fixed to a photographic scale of the optimized CRP1 for performance considerations. Thus, any structural and aero–structural tuning must be performed through tailoring of the composite laminates, including ply shapes and orientation angles.

As with the SRP scale model test case of Section 4.1.3, all scale model rotor performance parameters are contained within the objective function, which is now a summation over both of the rotor stages, as detailed in Section 3.9.2. Thus, the only constraints for this optimization (never active in this validation case) are the ply stress limits, to ensure test–worthiness.

For this validation case, it was decided to attempt construction of a 1/6 size scale model of the optimized CRP1, while minimizing the frequency differences between the two constructions. The exterior shape of the scale model was defined by updating the CRP1 design curves to their optimized configuration. Utilizing the proper scaled blade tip chord, STAT then generated the scaled blade shapes.

A laminated composite construction similar to that of the SR7a was employed for the scale model blades, using a fiberglass shell on alternating glass and graphite plies, with the innermost fiberglass glued to a titanium spar. Gaps are filled with glue.

The design variables, listed in Table 15, allow for modification of the interior construction of the composite airfoils by reshaping the graphite plies and the spar. A total of 35 design variables were employed for this test case, making this the largest STAT optimization performed to date.

For the objective of the scale model optimization, it was chosen to minimize the fractional frequency deviations for each of the two rotors between full size and scaled size, over the first five natural modes. Actually, the originally configured scale model geometry gave quite good initial frequency correlation, thus limiting the performance of the optimization capability. Nonetheless, an optimization was performed, with a resulting 15 percent improvement in frequency correlation. The optimization took a total of 285 design evaluations, using 7 complete design moves, and reached a converged optimum design. The final design variable values are listed on Table 16.

The frequency similarity based objective function values, along with the component frequencies, are listed on Table 17. The initial configuration for the scale model system gave good frequency correlation. The optimized system further improved the correlations.

Table 15 Scale Model CRP Design Variables

Design Variable	*% Span Location*	*Lower and Upper Limit*
Graphite Ply 1:		
Lower Cutoff		*−1 to +1*
Upper Cutoff		*−1 to +1*
Ply Angle		*−90 to +90 degrees*
Meanline Location	*30*	*−0.25 to +0.25*
	60	*−0.25 to +0.25*
	90	*−0.25 to +0.25*
Chordwise Extent	*30*	*−0.25 to +0.25*
	60	*−0.25 to +0.25*
	90	*−0.25 to +0.25*
Graphite Ply 2:		
Lower Cutoff		*−1 to +1*
Upper Cutoff		*−1 to +1*
Ply Angle		*−90 to +90 degrees*
Meanline Location	*35*	*−0.25 to +0.25*
	60	*−0.25 to +0.25*
	85	*−0.25 to +0.25*
Chordwise Extent	*35*	*−0.25 to +0.25*
	60	*−0.25 to +0.25*
	85	*−0.25 to +0.25*
Graphite Ply 3:		
Lower Cutoff		*−1 to +1*
Upper Cutoff		*−1 to +1*
Ply Angle		*−90 to +90 degrees*
Meanline Location	*30*	*−0.25 to +0.25*
	47.5	*−0.25 to +0.25*
	60	*−0.25 to +0.25*
Chordwise Extent	*30*	*−0.25 to +0.25*
	47.5	*−0.25 to +0.25*
	60	*−0.25 to +0.25*
Spar:		
Upper Cutoff		*−1 to +1*
Meanline Location	*25*	*−0.25 to +0.25*
	50	*−0.25 to +0.25*
	75	*−0.25 to +0.25*
Chordwise Extent	*25*	*−0.25 to +0.25*
	50	*−0.25 to +0.25*
	75	*−0.25 to +0.25*
Fill:		
Lower Cutoff		*−1 to +1*

Table 16 Optimum Scale Model CRP

Design Variable	*% Span Location*	*Design Variable Change*
Graphite Ply 1:		
Lower Cutoff		*0.013165*
Upper Cutoff		*0.027255*
Ply Angle		*0.050436*
Meanline Location	*30*	*−0.045404*
	60	*−0.030971*
	90	*−0.018440*
Chordwise Extent	*30*	*0.016945*
	60	*0.025627*
	90	*0.048033*
Graphite Ply 2:		
Lower Cutoff		*0.007975*
Upper Cutoff		*0.025680*
Ply Angle		*0.046841*
Meanline Location	*35*	*0.006383*
	60	*−0.053419*
	85	*−0.095086*
Chordwise Extent	*35*	*0.014481*
	60	*−0.046894*
	85	*−0.036355*
Graphite Ply 3:		
Lower Cutoff		*0.008776*
Upper Cutoff		*0.017896*
Ply Angle		*0.050115*
Meanline Location	*30*	*0.014423*
	47.5	*0.090104*
	60	*−0.008475*
Chordwise Extent	*30*	*0.008042*
	47.5	*0.009984*
	60	*0.004529*
Spar:		
Upper Cutoff		*0.022765*
Meanline Location	*25*	*−0.007160*
	50	*−0.048541*
	75	*0.038536*
Chordwise Extent	*25*	*0.007792*
	50	*0.010713*
	75	*0.031805*
Fill:		
Lower Cutoff		*0.020743*

Table 17 Scale Model CRP Frequency Correlation

	Base Blade Frequency (cps)	*Scaled Base Frequency (cps)*	*Original Scale Model Frequency (cps)*	*Optimum Scale Model Frequency (cps)*
Front Blade				
1	*33.4*	*193.6*	*197.9*	*202.9*
2	*85.1*	*500.1*	*496.7*	*510.8*
3	*113.0*	*664.1*	*599.3*	*604.2*
4	*123.6*	*726.4*	*743.6*	*742.6*
5	*174.1*	*1023.2*	*948.9*	*964.2*
Rear Blade				
1	*33.9*	*199.2*	*202.8*	*202.9*
2	*85.4*	*501.9*	*442.3*	*445.2*
3	*101.1*	*594.2*	*544.2*	*546.6*
4	*110.1*	*647.0*	*754.0*	*737.0*
5	*173.7*	*1020.8*	*893.7*	*894.0*
		Objective Function:	*0.0798*	*0.0678*

5. COMPUTATIONAL EFFICIENCY

5.1 Warm Start Finite Element Analysis

During a STAT optimization, many gradient evaluations are necessary, especially for optimizations with a large number of variables, such as the SR7 and SR7a. For each gradient evaluation, one variable is slightly perturbed from its latest design value while all the other variables remain unchanged. Thus, the blade has changed very little since the last design evaluation was made by ADS. Therefore, it is reasonable to assume that the blade deflections calculated from the previous gradient evaluation function call are very similar to those to be calculated by the finite element analysis of the current gradient evaluation.

Since the approximate finite element analysis of STAT requires the application of geometric nonlinear analysis to analyze highly swept fan blades, an iterative solution technique is required which simply calculates displacements necessary to balance all external loads. This is done by continually updating the stiffness matrix until an equilibrium state has been found. It has been found that a significant amount of time can be saved by simply initiating the analysis for the current design at the converged displacement solution of the previous design. This version of the finite element analysis is termed a 'warm' start as opposed to a 'cold' start analysis, which starts with the linear solution of an undeformed blade.

Occasionally, the 'warm' start analysis may fail because the gradient step made by ADS perturbed the design too much, then, a singular matrix will develop. The singular matrix development will signal the STAT finite element code to start again and run a 'cold' start analysis. Therefore, little time is wasted and the STAT optimization continues undisturbed. However, it should be noted that if a cold start is required on a gradient evaluation, the gradient step size is likely too large for that particular variable and could cause inaccurate gradients to be evaluated and subsequently used by ADS in performing its optimization.

5.2 ADS Optimization Scheme

The choice of the proper optimization scheme to be used for a particular STAT application depends on the nature of the problem. The SR7 and 18E design test cases represented tightly constrained problems, whereas the SR7A aeroelastic model test case represented the unconstrained tailoring of a blade.

The ADS 'Method of Feasible Directions' (scheme 0 4 8) and 'Modified Method of Feasible Directions' (scheme 0 5 8) have proven to be the most effective algorithms for solving tightly constrained problems such as the optimization of the LAP blades, SR7 and 18E. For these particular cases, the driving power was constrained to within 1 percent of 2592 hp and it was discovered that for such a tight equality constraint, the 0 5 8 method proved to move more efficiently toward an optimum design than the 0 4 8 method. This is due to the different manners the methods have when the problem has encountered a constraint. The 0 4 8 method 'bounces' off the constraint wall, whereas the 0 5 8 method uses the constraint gradient to move along the constraint boundary and thus reaches the optimum sooner.

The ADS algorithm 'Broydon–Fletcher–Goldfarb–Shanno' (BFGS) variable metric method for unconstrained minimization was found to be the most suitable method for solving the tailoring problem of the SR7A aeroelastic scale model. The objective function of the aeroelastic scale model test case was defined as the square of differences between the model and the SR7 blade design for static and dynamic characteristics such as mass distribution, static tip deflection, mode shapes and frequencies. Therefore, by theory the tailored SR7a would take on the identical aeroelastic properties of the full–scale SR7 design which satisfied all of the necessary constraints.

5.3 Optimization Computer Time Estimation

The execution time for a particular STAT optimization analysis is dependent upon several factors of which the most important are the number of design variables, the number of blade material layers, the blade nonlinear characteristics, and obviously, the number of design step iterations required to find an optimum design.

The STAT optimizer requires a function call for each variable to determine objective function and constraint gradients. Using these gradients, ADS starts varying the design and each time the design must be evaluated, which requires another function call. For the ADS 'Method of Feasible Directions' (0 4 8 or 0 5 8), about 3 to 5 function evaluations are necessary for each design iteration, whereas for the 'BFGS' method about an average of 5 function calls can be assumed. Additionally, design step function calls require a 'cold start' finite element analysis because the change in the blade design may be large but, the gradient evaluation function calls, which should represent small perturbations in the blade design, require only a 'warm start' finite element analysis.

The central processing unit (CPU) time necessary for the STAT approximate analysis loop for the SR7 and the SR7a run on the PWA IBM 3090 is as follows:

		warm loop	cold loop
SR7	7 layers	12.5 sec.	22.8 sec.
SR7a	23 layers	22.2 sec.	30.5 sec.

The differences stem from the pre– and post–processing time required for the additional composite layers of the aeroelastic scale model. Typically, only 3 to 4 CPU seconds are required by all of the remaining routines which include the aerodynamic, flutter, noise, once–per–revolution forced response, and ADS algorithms. Therefore, the benefit of the 'warm' start finite element capability is quite significant.

6. REFERENCES

1. Vanderplaats, G. N., Numerical Optimization Techniques for Engineering Design: With Applications, McGraw–Hill (1984).

2. Vanderplaats, G. N., H. Sugimoto and C. M. Sprague, "ADS–1: A New General Purpose Optimization Program," AIAA 24th Structures, Structural Dynamics and Materials Conference, Lake Tahoe, Nevada, May 1983.

3. Brown, K. W., Structural Tailoring of Advanced Turboprops (STAT) User's Manual, NASA CR–187101, November 1991.

4. Brown, K. W., Structural Tailoring of Advanced Turboprops (STAT) Programmer's Manual, NASA CR-191018, March 1992.

5. Jones, R. M., Mechanics of Composite Materials, Scripta Book Co., Washington, D. C., 1975.

6. MacNeal, R. H., "A Simple Quadrilateral Shell Element," *Computers & Structures*, Vol. 8, Pergamon Press, Great Britain, 1978, pp. 175–183.

7. Guyan, R. J., "Reduction of Stiffness and Mass Matrices," *AIAA Journal*, Vol. 3, 2, February 1965.

8. MacNeal, R. H., The NASTRAN Theoretical Manual, NASA Sp–221 (01), April 1972.

9. Zienkiewicz, O. C., The Finite Element Method, 2nd Ed., McGraw–Hill (1977).

10. Tsai, S. W. and Wu, E. M., "A General Theory of Strength for Anisotropic Materials," *J. Composite Materials*, Vol. 5 (January 1971), pp 58–80.

11. Thompson, William T., Theory of Vibration with Applications, Prentice–Hall Inc., Englewood Cliffs, New Jersey, 1972.

12. Egolf, T. A., O. L. Anderson, D. E. Edwards, A. J. Landgrebe, "An Analysis for High Speed Propeller–Nacelle Aerodynamic Performance Prediction," Volumes I, II, United Technologies Research Center, R79–912949–19, June 1979.

13. Borst, H. V., "Summary of Propeller Design Procedures and Data," USAAMRDL TR 73–34A, November 1973.

14. Goldstein, S., "On the Vortex Theory of Screw Propellers," Royal Society (London) Proceedings, Vol. 123, No. 792, April 6, 1929.

NASA
National Aeronautics and Space Administration

Report Documentation Page

1. Report No.	2. Government Accession No.	3. Recipient's Catalog No.
NASA CR–191017		

4. Title and Subtitle	5. Report Date
Structural Tailoring of Advanced Turboprops (STAT) Theoretical Manual	October 1992
	6. Performing Organization Code

7. Author(s)	8. Performing Organization Report No.
K. W. Brown	PWA–5767–109
	10. Work Unit No.

9. Performance Organization Name and Address	11. Contract or Grant No.
UTC–Pratt & Whitney 400 Main Street East Hartford, Connecticut 06108	NAS3–23941
	13. Type of Report and Period Covered
12. Sponsoring Agency Name and Address	Theoretical Manual
NASA–Lewis Research Center 21000 Brookpark Road Cleveland, Ohio 44135	14. Sponsoring Agency Code

15. Supplementary Notes

Program Manager: D. Hopkins
NASA–Lewis Research Center

16. Abstract

This manual describes the theories included in the Structural Tailoring of Advanced Turboprops (STAT) computer program, which was developed to perform numerical optimizations on highly swept propfan blades. The optimization procedure seeks to minimize an objective function, defined as either direct operating cost or aeroelastic differences between a blade and its scaled model, by tuning internal and external geometry variables that must satisfy realistic blade design constraints. The STAT analyses include an aerodynamic efficiency evaluation, a finite element stress and vibration analysis, an acoustic analysis, a flutter analysis, and a once–per–revolution (1–P) forced response life prediction capability. The STAT constraints include blade stresses, blade resonances, flutter, tip displacements and a 1–P forced response life fraction. The STAT variables include all blade internal and external geometry parameters needed to define a composite material blade. The STAT objective function is dependent upon a blade baseline definition which the user supplies to describe a current blade design for cost optimization or for the tailoring of an aeroelastic scale model.

17. Key Words (Suggested by Author(s))	18. Distribution Statement
Approximate Analysis; Mathematical Optimization; Objective Function; Refined Analysis; Input; Output	

19. Security Classif. (of this report)	20. Security Classif. (of this page)	21. No. of pages	22. Price
Unclassified	Unclassified	78	

NASA FORM 1626 OCT 86